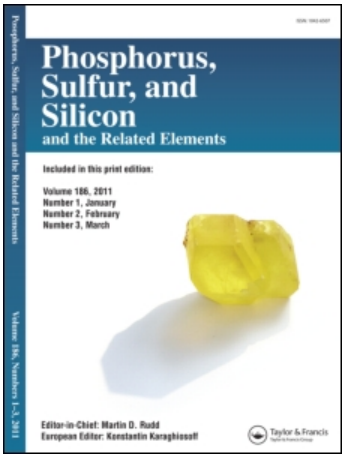

Phosphorus, Sulfur, and Silicon and the Related Elements
Publication details, including instructions for authors and subscription information:
http://www.informaworld.com/smpp/title~content=t713618290

Principles of Phosphorus Chemistry: Molecular States of Phosphorus Compounds - A Report on Gasphase Investigations [1-3]

Hans Bock[a]
[a] Institute of Inorganic Chemistry, University of Frankfurt Niederurseler Hang, Frankfurt/Main, West Germany

To cite this Article Bock, Hans(1990) 'Principles of Phosphorus Chemistry: Molecular States of Phosphorus Compounds - A Report on Gasphase Investigations [1-3]', Phosphorus, Sulfur, and Silicon and the Related Elements, 49: 1, 3 — 53
To link to this Article: DOI: 10.1080/10426509008038905
URL: http://dx.doi.org/10.1080/10426509008038905

Phosphorus, Sulfur, and Silicon, 1990, Vols. 49/50, pp. 3–53
Reprints available directly from the publisher
Photocopying permitted by license only

PRINCIPLES OF PHOSPHORUS CHEMISTRY:

MOLECULAR STATES OF PHOSPHORUS COMPOUNDS - A REPORT ON GASPHASE INVESTIGATIONS[1-3]

HANS BOCK
Institute of Inorganic Chemistry, University of Frankfurt
Niederurseler Hang, D 6000 Frankfurt/Main, West Germany

Dedicated to Professor Kurt Issleib on occasion of his 70th birthday

Abstract. An up-to-date concept of bonding in phosphorus compounds has to be based on the reality of molecular states. Molecules, which change their structure with energy, at present are best rationalized in terms of topology and symmetry, effective nuclear potentials and charge distribution. To reduce the complexity of the resulting manifold, comparison of equivalent states of chemically related molecules, based advantageously on quantum chemical calculations, is strongly recommended. Adding the time-scale, molecular dynamics within the numerous degrees of freedom become important, also as a basis to gain some understanding of the rather complex microscopic reaction pathways of medium-sized molecules. Examples are presented to illustrate the use of spectroscopic 'fingerprints' for the analysis and optimization of gasphase reactions as well as the benefit of inherent information on molecular states for the preparative phosphorus chemist. The catalytic dehydrochlorination of alkyldichlorophosphanes $RH_2C\text{-}PCl_2 \rightarrow RHC=PCl \rightarrow R\text{-}C\equiv P$ and their dechlorination on magnesium metal surface are discussed in some detail as well as the generation of other unsaturated phosphorus molecules like $Cl\text{-}P=O$, $Cl\text{-}P=S$, $Cl\text{-}P(=O)_2$,$Cl\text{-}P(=S)_2$ or $H_3C\text{-}P=CH_2$. Approximate energy hypersurface calculations for the gasphase equilibrium $P_4 \rightleftarrows 2\,P_2$ or for the unexpected dehydration $(H_3C)_2HP=O \rightarrow H_2O + H_3C\text{-}P=CH_2$, which includes chemical activation, provide some insight into microscopic reaction pathways of phosphorus compounds.

CONTENTS

1. INTRODUCTION: FACETS OF MOLECULAR STATES - A SIMPLIFIED APPROACH

1.1. Molecular States: Measurement, Rationalization and Utilization

The structures of molecules and hence their properties will change with energy and especially on acquisition or loss of electrons. The individual state of molecule or a molecular ion is characterized by the energy differences from a preceding or to a subsequent state, by its respective charge distribution i.e. its structure and by its molecular dynamics. A multitude of measurement techniques available from the physical armoury provide information both on the energy differences between and the structures of invidual molecular states.[3]

For the preparative chemist, however, the molecular states and their properties (Figure 1), which he measures day by day in order to identify, to analyze and to characterize his compounds,[1,3] obviously are often difficult to rationalize and, therefore, quite some information inherent in his spectra remains unused. On the other hand, a simplified molecular state approach, which e.g. largely neglects the rather complicated molecular dynamics, is readily available.[3] It could be used by the chemist for his own benefit in many ways, for instance,

- ▷ to compare 'equivalent states' of 'chemically related', preferentially iso(valence)electronic molecules, thus making use of the vast literature to stimulate his own research,
- ▷ to disentangle the multitude of known compounds and to rationalize their numerous properties by e.g. defining 'parent systems' and substituent perturbations,[1,3,4] and
- ▷ to develop models based e.g. on topology and especially on symmetry considerations,[1,3,4] introducing in addition effective atomic potentials from relevant experimental energy data, as well as on approximate or more rigorous quantum chemistry calculations.

All of the above suggestions have been developed, are presently applied and will be further improved by many researchers in all fields of chemistry and thus the purpose of my lecture only can be to demonstrate, how easily the simplified molecular state approach may be extended to include phosphorus chemistry at its present state of maturity and with respect to its tremendous future aspects. Therefore, please accept my recommendation of a 'molecular state magnifier' (Figure 2) to the preparative phosphorus chemist.

1.2. Properties of Molecules in Their Various States

A molecule, if energy is supplied to or withdrawn from it, will change into another state. If, in addition, electrons are acquired or released during this

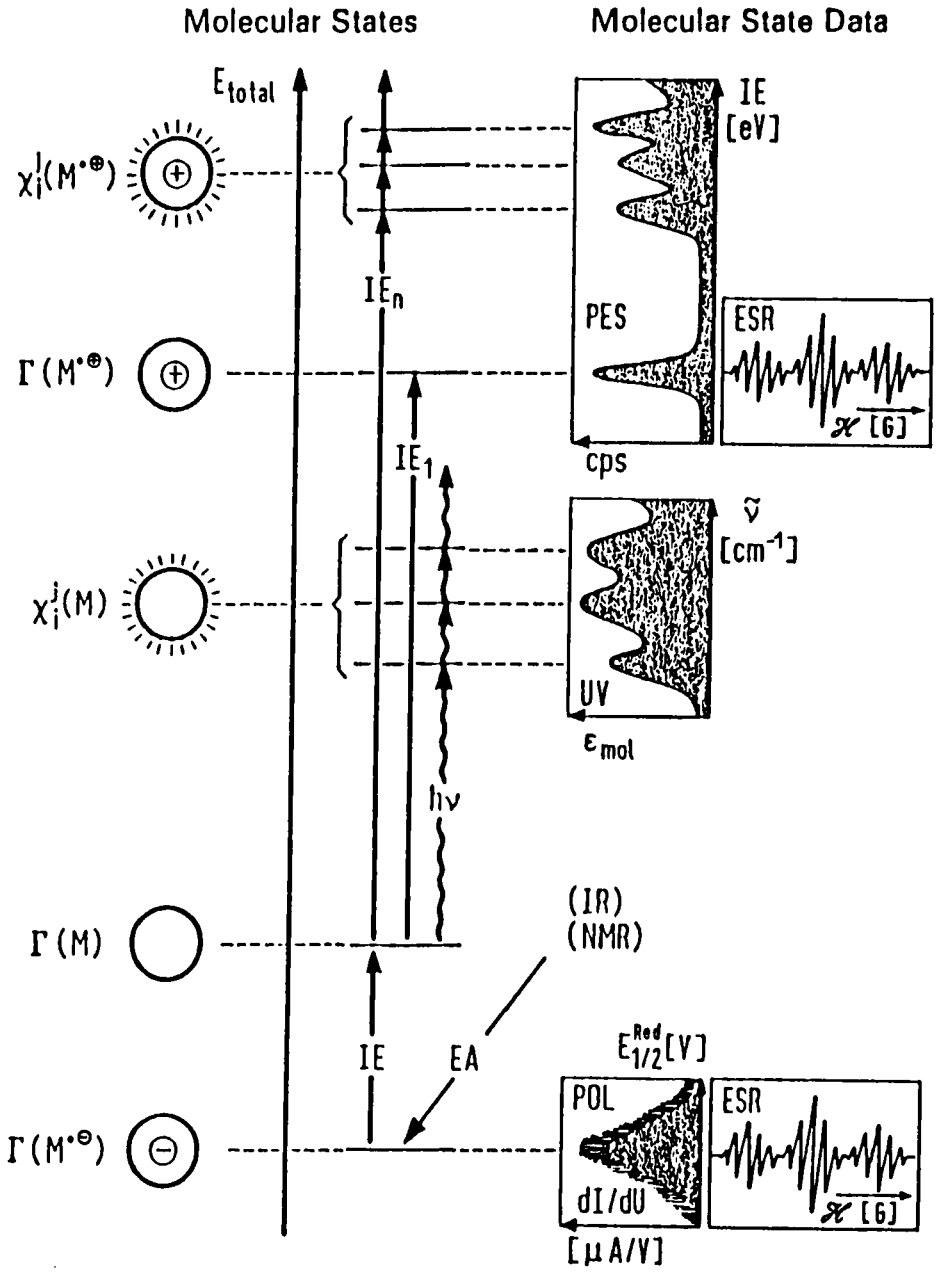

FIGURE 1. Selection from the multitude of molecular states comprising ground (Γ) and electronically (χ_i^j) as well as vibrationally (IR) excited states of a neutral molecule M, its radical cation $M^{\cdot\oplus}$ and its radical anion $M^{\cdot\ominus}$, together with basic information as supplied by UV or PE spectra in the gasphase or by ESR signal patterns or electrochemistry in solution (see text).

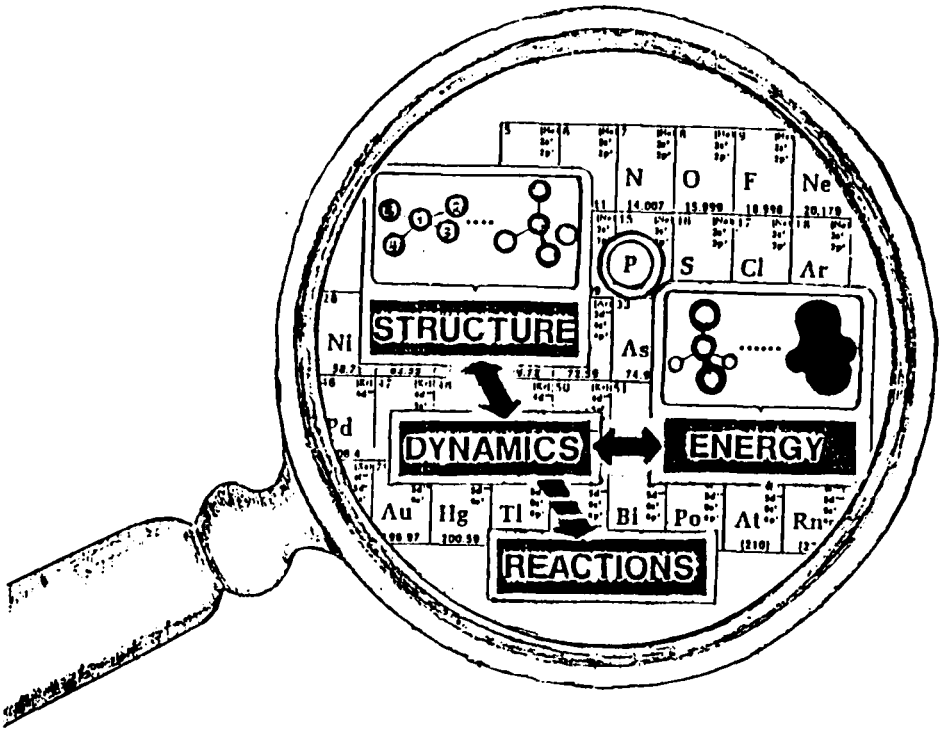

FIGURE 2. 'Molecular State Magnifier' for the preparative phosphorus chemist

transition, then molecular ions forms as new species, which may be radicals and which also exist in numerous states of various energies[1,3] (Figure 1).

The energy differences between molecular states can be measured by a variety of techniques (cf. examples given in Figure 1) and show that the total energy of the individual states[1,3] of a molecule M increases from those of its stable radical anion $M^{\cdot\ominus}$ - formed, if M exhibits a negative electron affinity - via those of the neutral molecule M to those of its radical cation $M^{\cdot\oplus}$ (Figure 1). As concerns their different structures, there are in addition to diffraction and microwave spectroscopic methods, many measurement techniques, which yield - for instance, via selection rules or from signal patterns for equivalent centers - information on their respective symmetry. And, not to forget, more sophisticated quantum chemical calculations do also provide reliable structural estimates,[3] which are extremly valuable whenever an experimental determination is impossible.

Nevertheless, the multitude of states for any individual molecule, especially on inclusion of its dynamics, and the numerous properties of every single state as accessible by measurement, is overwhelming and largely outside the focus of interest of the synthetically-minded chemist. Let us ask, therefore, what demands he would place on a suitable model[1,3] for molecular states? Above all, it

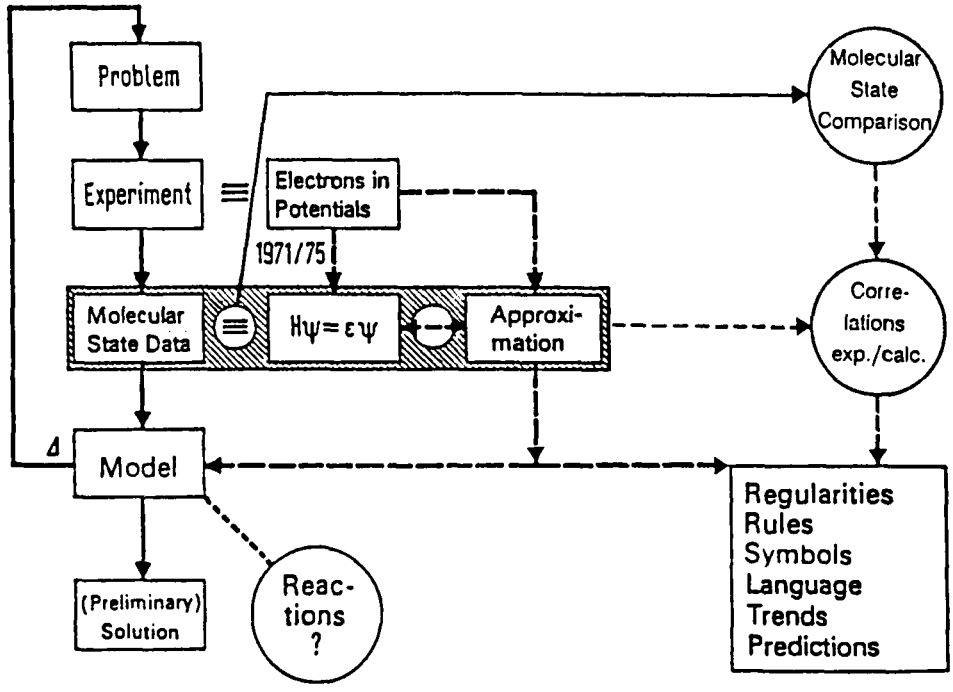

FIGURE 3. Scheme proposing the rationalization of experimental molecular state data by comparison with equivalent ones of chemically related molecules as well with the results of more rigorous or even approximate quantum chemical calculations. Suitable models established close to experiment will especially help to avoid language problems arising from rather chaotic bonding discussions based on artificially subdividing molecular entities by identifying topological connectivity symbols with exactly two electrons (see text).

must be close to experiment and to his expertise, allow to compare chemically related compounds - as he would define them -, use transparent parameters and, last but not least, should be as general and as flexible as possible. Most of these demands are met by the scheme[3] displayed in Figure 3. Accordingly, experimental investigation of a chemical problem yields molecular state data, which for rationalization are best compared with equivalent ones of chemically related compounds. Often quantum chemical calculations - decribing the behaviour of electrons in given potentials, highly correlated for small molecules and less rigorously for larger ones, are quite helpful to predict or to reproduce facts. And, especially, they stimulate preparative chemists to develop models close to experiment. These, in return, should allow to detect and to verify regularities and trends. In addition, it is sincerely hoped that the quantum chemical language, treating molecules and their states as entities in terms of their total energy, their charge distribution and their dynamics will replace discussions of 'atoms in

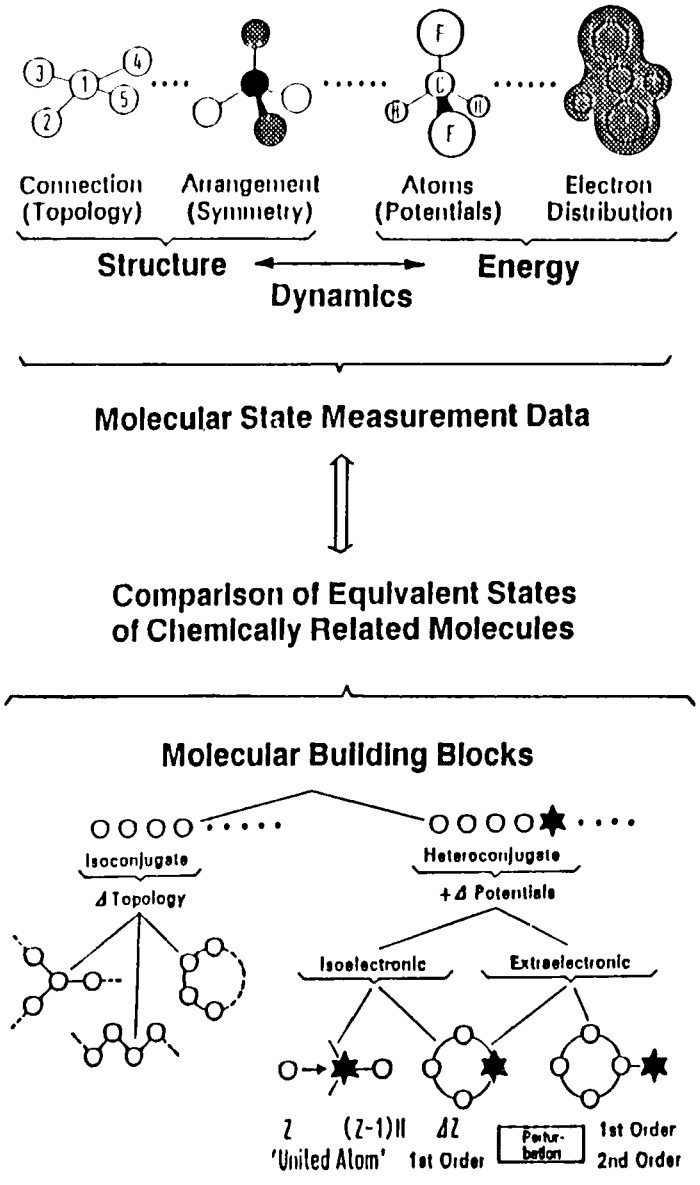

FIGURE 4. Simplified approach to rationalize properties of molecular states by emphasizing connectivity, spatial arrangement, effective nuclear potentials and electron distribution as well as relationships between structure and energy as coupled by molecular dynamics. The comparison of equivalent states of chemically related molecules advantageously starts with the definition of molecular 'building blocks', which, if isoconjugate, may be rationalized in terms of their changing topology and, if heteroconjugate, may be discussed including the potential differences into first and second perturbation arguments (see text).

molecules' and the 'bonding between them' by e.g. undefined electronegativities, fictitious d-orbitals and resonance energies or non-experimental concepts like 'soft and hard' acid and bases (Figure 3). Improved knowledge concerning the dynamics of larger molecules with numerous degrees of freedom should also enhance our rather rudimentary understanding of the unknown microscopic pathways of chemical reactions.[5]

A useful simplified approach to rationalize properties of molecular states (Figure 4: top) - proposed already 12 years ago[3] - starts from the topology of the molecular skeleton unfolded to the spatial arrangement as denoted by symmetry. Into this structural framework, energy aspects are introduced by defining effective potentials for the individual centers, representing various kinds of atoms, in such a way that the resulting electron distribution reproduces all essential details of the respective molecular structure. Of special importance is the relationship between structure and energy: there is no change in energy - especially, if coupled to addition or loss of electrons - without a corresponding change in structure and vice versa.[3] In some cases - as will be illustrated e.g. in the chapter 6 - certain aspects of molecular dynamics might be included. Above all, for the preparative chemist such an approach (Figures 3 and 4) must permit the comparison of experimental data within the series of compounds he investigates.

As concerns the comparison of equivalent states of chemically related molecules, practically every chemist attempts to organize his set of individual compounds by some definition of chemical relatedness, e.g. by principles of homology or by substituent effects.[1,3,6] Often, a definition of 'molecular building blocks' and their combination within a 'molecules in molecule' treatment (Figure 4: bottom) is recommended for molecular state comparison: Depending upon the relative change, the distinction between iso- and hetero-conjugate, and between iso- and extra-electronic systems is of course a flexible one. The extent of perturbation[4] often also determines the scope of a model (Figure 3), and within this scope, its quality, i.e. the deviations in correlations between observed and calculated quantities.

1.3. Investigations of the Frankfurt PES and ESR/ENDOR Group

Contributions along these lines (chapter 1.2) and over the years by the Frankfurt PES and ESR/ENDOR group concerning phosphorus compounds as part of our investigations on main group element chemistry comprise:[6]

- ▷ relations between color and constitution of violet phosphorus azo compounds $R_2(X)P\text{-}N=N\text{-}P(X)R_2$,[7]
- ▷ the assignment of numerous PE spectra of phosphorus compounds including those of ylides,[8] polyphosphor rings like $(PCH_3)_5$[9] or clusters

like $P_7(SiR_3)_3$ [9] by Koopmans' correlation, $IE_n^v = -\varepsilon_j^{SCF}$, with SCF eigenvalues or by molecular state comparison,

- ▷ cyclovoltammetric measurements of organophosphorus π systems[10] and generation as well as ESR/ENDOR characterization of their radical cations[11] and radical anions,[12]
- ▷ the thermal generation of unsaturated phosphorus molecules such as $P\equiv C\text{-}C\equiv P$,[13] $P\equiv P$,[14] Cl-P=O and Cl-P=S,[15] Cl-$P(=O)_2$ and Cl-$P(=S)_2$,[16] as well as $H_3C\text{-}P=CH_2$,[17,18] under (nearly) unimolecular conditions and their unequivocal identification by photoelectron spectroscopic ionization patterns,[19]
- ▷ the calculation of semiempirical energy hypersurfaces[20] to approximate dynamic phenomena[9] or facets of microscopic reaction pathways,[14,18,20,21]
- ▷ the optimization of the heterogeneously catalyzed dehydrochlorination of alkylphosphorus chlorides[22] by real-time photoelectron spectroscopic gas analysis.[19,23] and
- ▷ the thermal elimination of water from dimethylphosphane oxide $(H_3C)_2HP=O$ to $H_3C\text{-}P=CH_2$ in the gasphase, which is interpreted with chemical activation along the reaction pathway.[18,21]

Selected examples from these research projects - all of them concerning gasphase investigations using advantageously photoelectron spectroscopy for real-time analysis in the flow systems - shall be presented in more detail as a further recommendation to the preparative phosphorus chemist that he uses molecular state fingerprints not only for analytical purposes, but also rationalizes within a simplified approach[1,3,6] (Figure 2) more of the inherent information.

To begin with, a cooperation with industry to develop a dehydrochlorination catalyst[22] for alkyl phosphorus chlorides will be reported as a first example.

2. THERMAL AND HETEROGENEOUSLY CATALYZED DEHYDROCHLORINATION OF ALKYLDICHLOROPHOSPHANES

2.1. Photoelectron Spectroscopic Real-Time Gas Analysis

In general, the combination of preparative main group chemistry with an appropriate physical measurement method and accompanying quantum chemical calculations proves to be advantageous for various purposes. But there is hardly any more successful technique than photoelectron spectroscopy to generate novel short-lived i.e. rather reactive molecules in the gasphase under reasonably high dilution, to optimize the respective reaction conditions by their spectroscopic signal intensities and to identify them instantly either by their precalculatable molecular state fingerprints or by comparison with those of chemically related known analogues.[19,23] The advantages of PES real-time gas analysis for both

monitoring thermal reaction conditions and to immediately characterize the novel short-lived molecules generated, is largely due to the fact that all radical cation states of a molecule are observed, unimpeded by any selection rules.[2,3] The ionisation band patterns recorded, in addition, can be calculated for smaller molecules using highly correlated wave-functions and for larger ones approximated via Koopmans' correlation, $IE_n^v = -\varepsilon_n^{SCF}$, by SCF eigenvalues. In essence, it is the intimate relationship between experimentally determined data and results from quantumchemical models, which provides a wealth of information.[2,3]

PES real-time gas analysis has repeatedly been used to optimize heterogeneously catalyzed reactions:[19,23,24] with only millimole quantities of the reactands and within 6 - 8 hours, the temperature dependence between 300 K and 1400 K can be determined. Screening of potential catalysts and their fine-tuning thus is usually accomplished within a few months time. As a special advantage for poisonous, pyrophoric and partly extremely odorous phosphorus compounds, it shall be pointed out that they can be safely handled within the vacuum-line system used (Figure 5).

2.2. The H_3CH_2C-PCl_2 Model Reaction: Catalyst-Screening and Fine-Tuning

Among other phosphorus projects, recently a heterogeneous catalyst for the gasphase dehydrochlorination of alkyldichlorophosphanes has been developed[22]. The objective of the investigation, the model reaction chosen and the apparatus used, the structure and dynamics of the precursor H_3CH_2C-PCl_2 as well as the PES gas analysis together with the assignment of the characteristic n_P and n_{Cl} ionisation bands are all outlined in Figure 5. Also in a self-explanatory way, the thermal decomposition of ethyldichlorophosphane and the fractionation of the resulting thermolysis products to yield pure $(H_3C)HC=PCl$ and H_3C-$C\equiv P$ [25-27] are shown in Figure 6 and the catalyst screening as well as its fine-tuning in Figures 7 and 8.

The thermolysis of H_3CH_2C-PCl_2 at temperatures above 820 K (Figure 6) leads to a mixture of products from predominantly two competing fragmentations: the elimination of ethen and of HCl.[22,27] The search for a heterogeneous catalyst, therefore, aims at both a lower reaction temperature and especially a higher dehydrochlorination selectivity. The catalyst screening (Figure 7) and fine-tuning (Figure 8) of the model reaction $(H_3C)H_2C$-$PCl \rightarrow (H_3C)HC=PCl \rightarrow H_3C$-$C\equiv P$ chosen (Figure 6) allowed to optimize the heterogeneously catalyzed HCl elimination from alkyldichlorophosphanes. The results obtained by using the most elegant real-time PES gas analysis i.e. the intensity changes in the molecular ionization 'fingerprints' from those of the educt into those of the products may be summarized and commented on as follows:

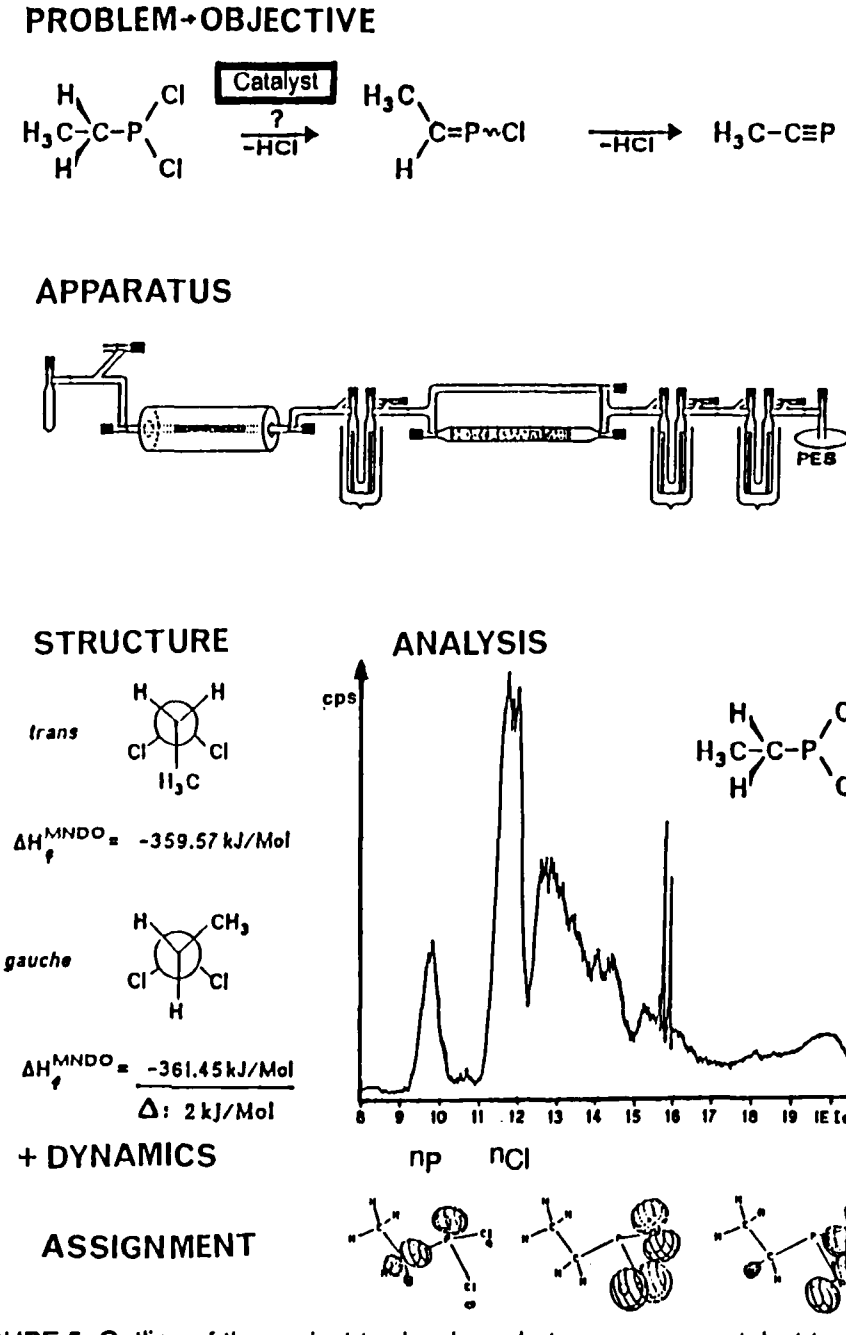

FIGURE 5. Outline of the project to develop a heterogeneous catalyst to split off HCl from alkyldichlorophosphanes at low temperature: the model reaction chosen (cf. Figure 6), the apparatus connected to a PE spectrometer and consisting of a horizontal reactor, intense cooling traps with bypass lines as well as an absorber tube, structure and dynamics calculated for $H_3CH_2C\text{-}PCl_2$ and its PE spectrum with assignment of the characteristic n_P and n_{Cl} ionisations.

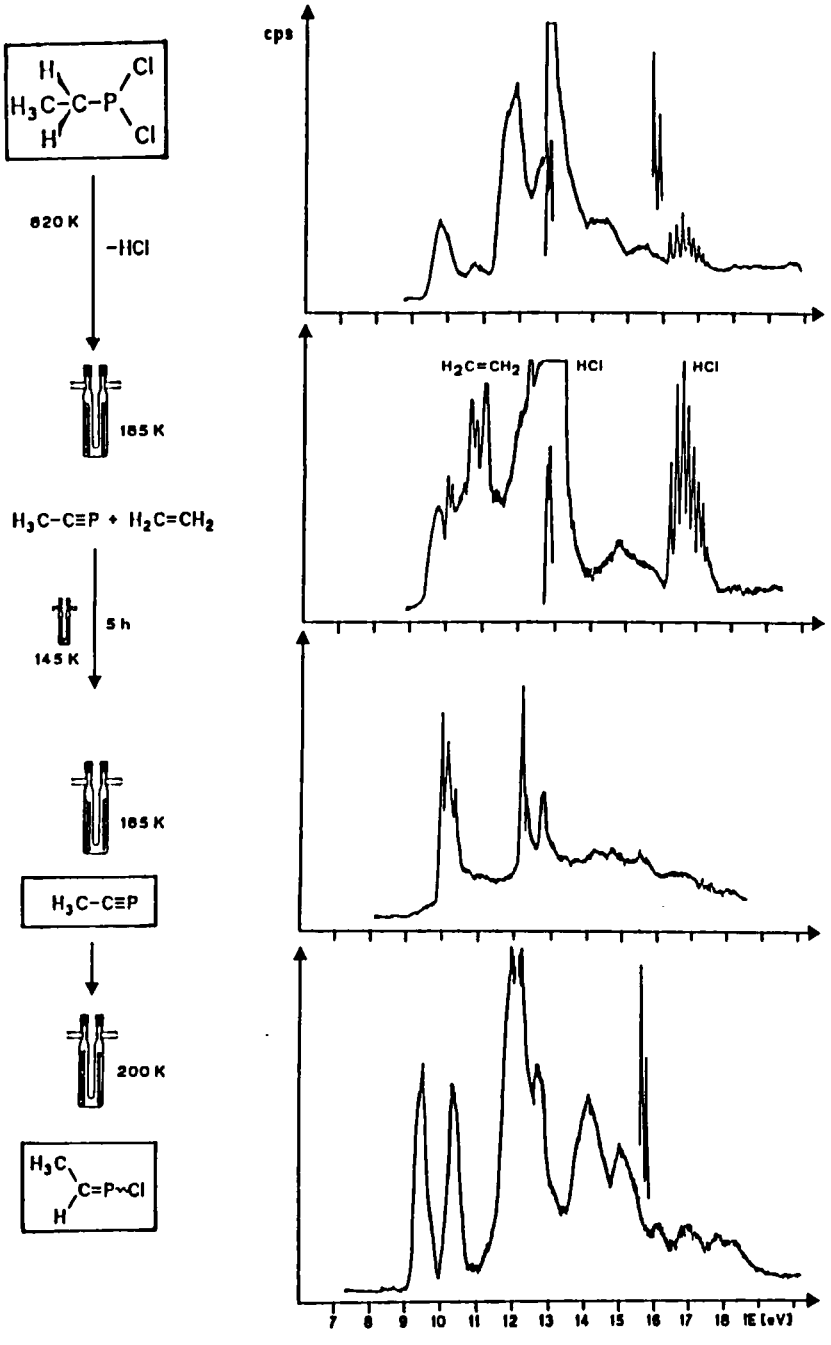

FIGURE 6. He(I)PE spectra for the thermal HCl elimination from ethyldichlorophosphane in a horizontal reactor (Figure 5) filled with quartz wool at 820 K and fractionation of the fragment products using intense cooling traps (Figure 5) with bypass lines as well as of the purified compounds $(H_3C)HC=PCl$ and $H_3C\text{-}C\equiv P$ isolated.

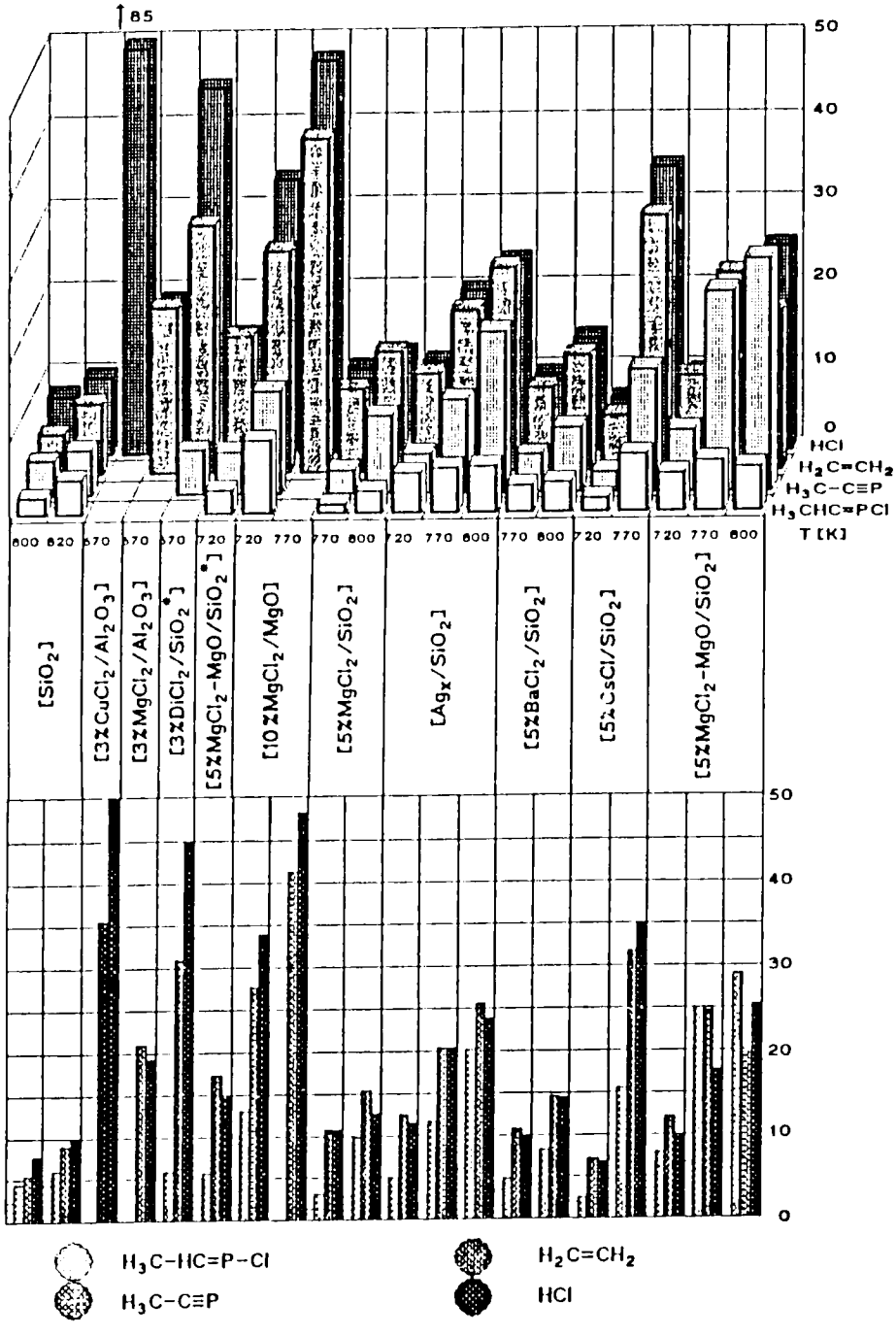

FIGURE 7. Catalyst screening for the heterogeneous HCl elimination from ethyldichlorophosphane: Temperature-dependent yields of the products $(H_3C)HC{=}PCl$ and $H_3C\text{-}C{\equiv}P$ as well as $H_2C{=}CH_2$ and HCl at various catalysts.

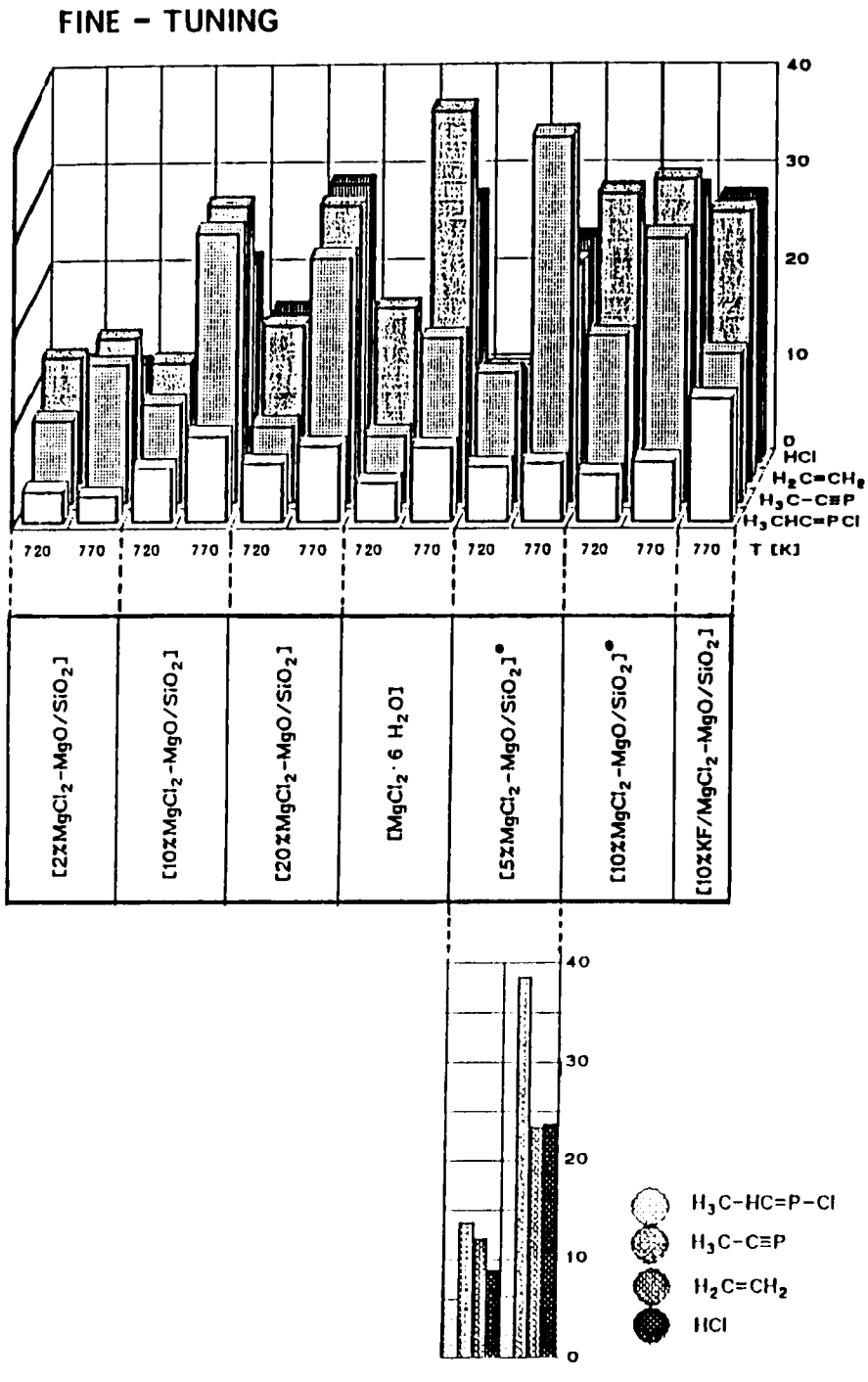

FIGURE 8. Fine-tuning of $MgCl_2$ (MgO) catalysts of varying composition and predominantly deposited onto quartz supports: Temperature-dependent yields of $(H_3C)HC=PCl$, $H_3C\text{-}C\equiv P$, $H_2C=CH_2$ and HCl (see text)

- ▷ Obviously, the activity of the most effective catalyst [$MgCl_2$-$MgO/SiO_2]_\infty$ (Figure 7) strongly depends on its $MgCl_2$ content (Figure 8), with an optimum for the lower temperature of 720 K within 5 to 10 % impregnation of the quartz wool support. Addition of 10 % KF promotor slightly increases the $(H_3C)_2HC=PCl$ yield (Figure 8).
- ▷ Relative to the thermal fragmentation on quartz wool (Figures 6 and 7), the average reaction temperature is lowered by about 150 K, which improves the yields of unsaturated phosphorus compounds from rather poor 10 % to about 50 % of isolated products, while the rate of the competing $H_2C=CH_2$ elimination is reduced from ~ 50 % to about 20 % (Figures 7 and 8).
- ▷ For the isolation of pure $(H_3C)HC=PCl$ and $H_3C\text{-}C\equiv P$, first the HCl formed has to be removed: according to our experience,[22,26] urotropine $(H_2C)_6(NH)_4$ proves to be an efficient absorber (cf. apparatus in Figure 5). The remaining reaction products are cool-trapped at 140 K and separated by fractionation into $H_3C\text{-}C\equiv P$ at 160 K and $(H_3C)HC=PCl$[22,27] at 190 K.

The photoelectron spectrum[22] of ethylenechlorophosphane (Figure 6),recorded for the first time,indicates the presence of the E isomer in addition to the dominant Z isomer,[27] which according to MNDO heats of formation is thermodynamically more stable by only 2 kJ/mol and separated by a low inversion barrier of only 29 kJ/mol.[22]

2.3. Isolation of Compounds $RR'C=PCl$ and $R\text{-}C\equiv P$

Summarizing, an active dehydrochlorination catalyst [$MgCl_2$-MgO/SiO_2] for alkyldichlorophosphanes has been developed (Figures 7 and 8), which lowers the HCl elimination temperatures selectively and thus reduces the rate of the otherwise dominant olefin split-off. From the resulting product mixtures, the respective alkylene chlorophosphanes $RR'C=PCl_2$ and alkylidine phosphanes $R\text{-}C\equiv P$ could be isolated by fractionate condensation (cf. apparatus with cooling traps in Figure 5). In the following, some details are given for both $(H_3C)_2C=PCl$ and $H_2C=PCl$:[22]

- ▷ The dehydrochlorination catalyst [10 % $MgCl_2$ - MgO/SiO_2] developed lowers the HCl elimination temperatures for a variety of compounds e.g. for $(H_3C)_3CCl$ to $(H_3C)_2C=CH_2$ by 350 K(!) to only 350 K i.e. 50 K above room temperature.[22] From isopropyldichlorophosphane, which on thermolysis above 820 K exclusively splits off propene, the novel compound isopropylene chlorophosphane (Figure 9) can be isolated:

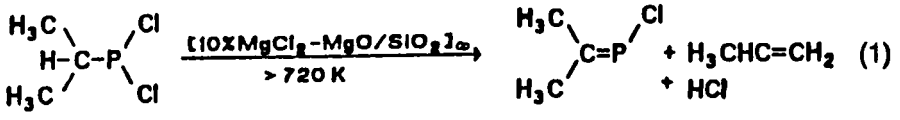

(1)

▷ On the other hand, methyldichlorophosphane and its 670 K dehydrochlorination products are further decomposed or polymerized on the catalyst surface. Therefore, both methylene chlorophosphane and methylidene phosphane are best generated thermally in an empty quartz tube heated above 1150 K and isolated by fractionate condensation:

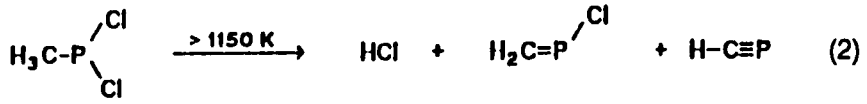

(2)

Altogether, the thermal generation of the rather reactive phosphorus compounds in the gasphase, their identification via individual radical cation state band patterns as well as their isolation using low temperature fractionation have been accomplished by following and optimizing each step with the help of real-time PE spectroscopic gas analysis.

2.4. Methyl Perturbation of $H_2C=PCl$

As pointed out in the beginning, spectroscopic 'molecular fingerprints' contain more information on the respective compounds than needed for their analytical identification. For example, radical cation state comparison of the chemically closely related methylene, ethylene and isopropylene chlorophosphanes (Figures 9) immediately allows to 'read off' the methyl group perturbations of the respective $M^{\cdot\oplus}$ states with predominant $\pi_{C=P}$, n_P and n_{Cl} contribution to the delocalization of the positive charge. Whereas the ionisations of both the phosphorus lone pair n_P in β position and the chlorine lone pairs n_{Cl} in γ position are shifted only slightly and to the same extent, one recognizes already from the increasing distance of the first two bands in the PE spectra (Figure 9) that the methyl substituent effect on the $\pi_{C=P}$ bond must be more pronounced. The perturbation parameter, $\Delta\pi_{C=P}$ ~ 0,4 eV, when compared to the differences in first ionisation energies between ethene and propene, ΔIE_1^v = 0,78 eV[28], indicates a 'weaker' and more polarized phosphaethylene π system, $>C^{(\delta\oplus)}=P^{(\delta\ominus)}Cl$ but matches, on the other hand, the ΔIE_1^v = 0,4 eV observed between benzene and toluene.[29] In terms of first order perturbation,[4] $\delta\varepsilon_J = c_{J\mu}\delta\alpha_{CH3}$, this infers for the $\pi_{C=P(Cl)}$ bond that the squared coefficient at the C center must be ~ 1/3, reduced relative to $c_{J\mu}$ = 1/2 in $H_2C=CH_2$.

Altogether - and at no additional cost -, looking at the analytical 'molecular fingerprints' again with the 'molecular state magnifier' for the preparative phosphorus chemist (Figure 2) provides an interesting insight into the electron density distribution of the phosphaethylene $H_2C=PH$ π system. The very appropriate comparison with the iso(valence)electronic parent compound ethylene $H_2C=CH_2$ indicates, in addition, why the smallest unsaturated organophosphorus compound with a single π bond might be as reactive and, therefore, short-lived as observed experimentally.[22,25]

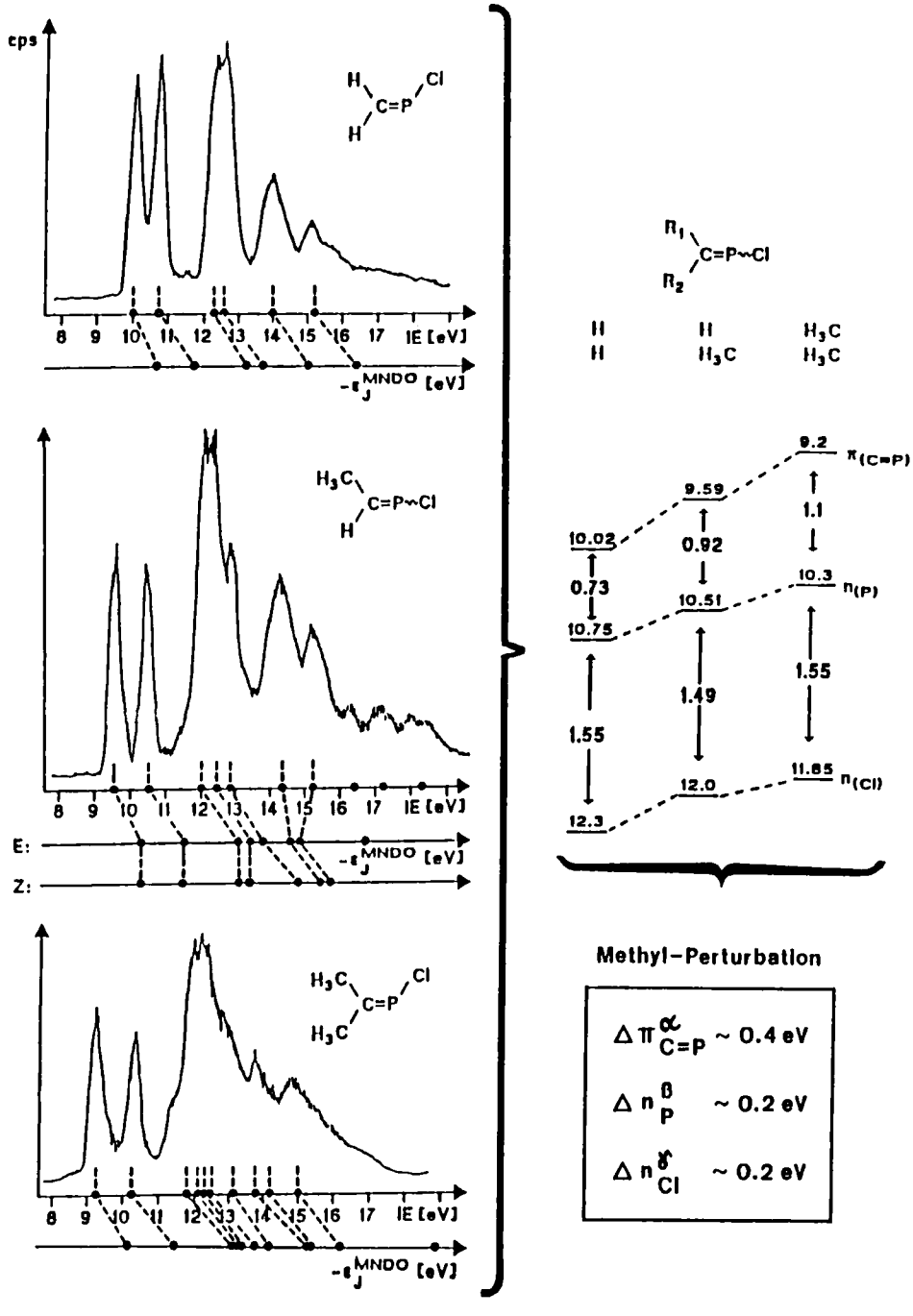

FIGURE 9. He(I)PE spectra of methylene, ethylene and isopropylene chlorophosphanes with assignment by Koopmans' correlation with MNDO eigenvalues, correlation diagram of their three lowest ionisation energies and methyl perturbation parameter for the respective $\pi_{C=P}$, n_P and n_{Cl} radical cation states (see text).

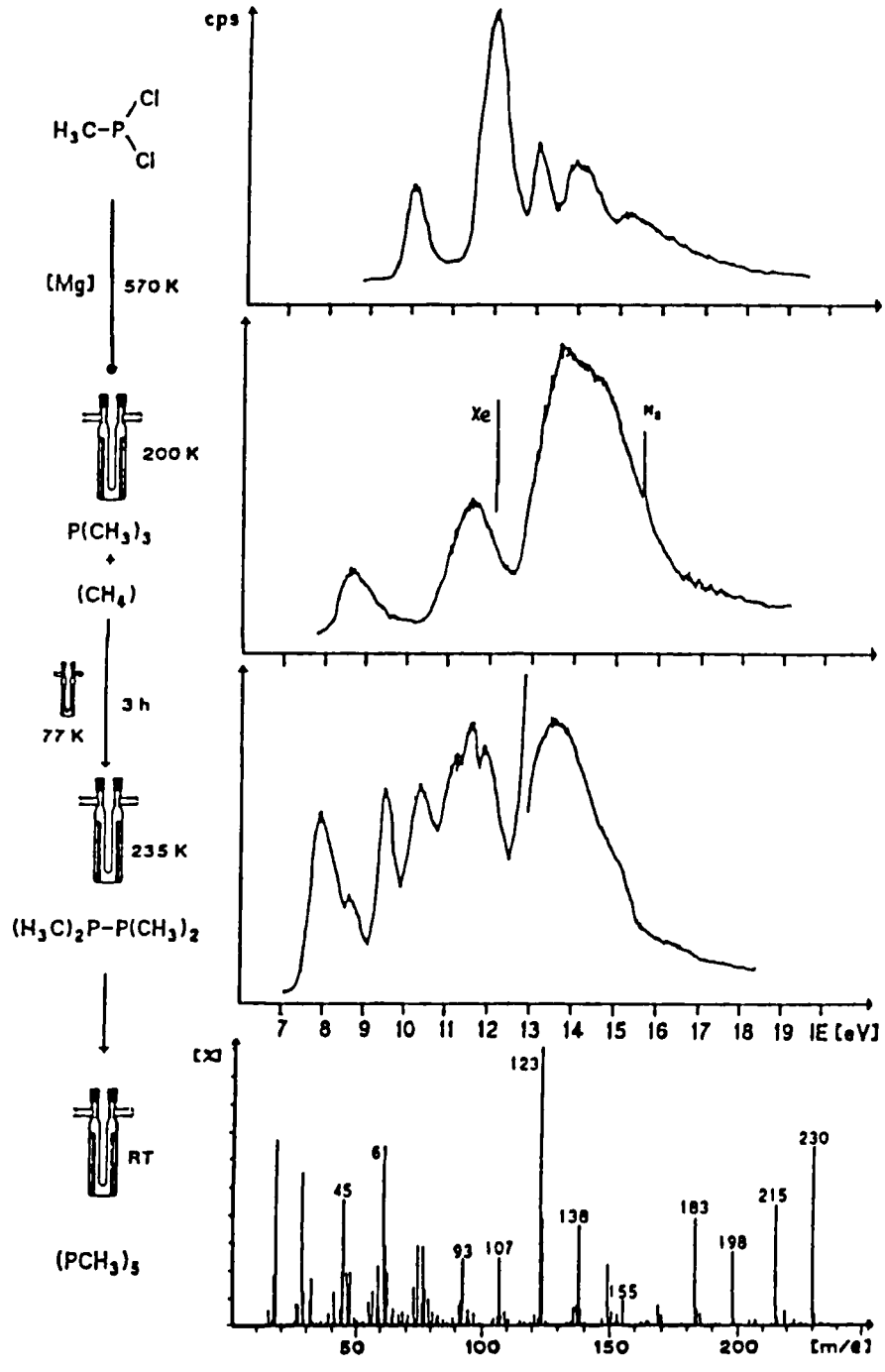

FIGURE 10. Reaction of gaseous $H_3C\text{-}PCl_2$ with Mg in a flow reactor with intense cooling traps connected to a high vacuum line and the PE spectrometer (cf. Figure 5) yielding a product mixture, from which after fractionation at the temperatures indicated, $P(CH_3)_3$, CH_4, $(H_3C)_2P\text{-}P(CH_3)_2$ and $(PCH_3)_5$ have been identified by the PES ionization and mass fragmentation patterns shown.

3. EVIDENCE FOR SURFACE PHOSPHINIDENE INTERMEDIATES [RP → Mg] IN THE HETEROGENEOUS DECHLORINATION OF ALKYLDICHLOROPHOSPHANES R-PCl_2 BY Mg METAL

In recent years, heterogeneous dehalogenation of a variety of phosphorus compounds with geminal halogens, has made accessible numerous unsaturated molecules containing phosphorus centers of low coordination number, e,g,[15,20,31]:

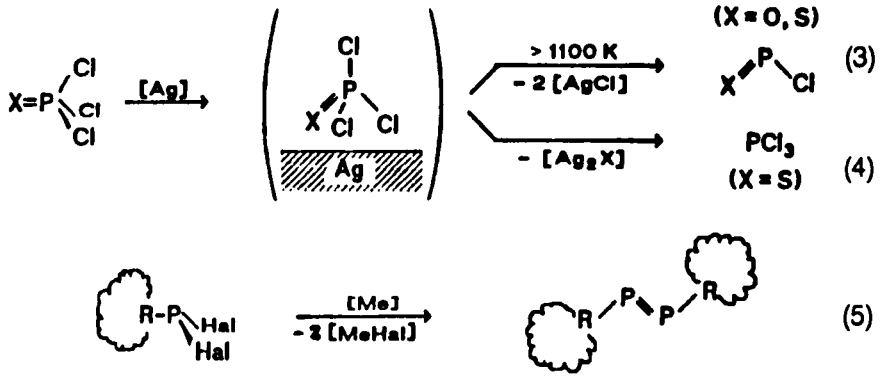

In contrast to the dechlorination of $O=PCl_3$ (3), which is based on the thermal instability of [Ag_2O] above 620 K and, therefore, exclusively yields O=P-Cl, the reaction of $S=PCl_3$ due to the higher decomposition temperature of [Ag_2S] produces a mixture of S=P-Cl and PCl_3 (4).[2] Although analogous evidence is lacking for a chemisorbed surface intermediate in the synthesis of kinetically stabilized diphosphenes RP=PR in solution,[31] the suspected phosphinidene intermediates RP, generated e.g. by R-$PHal_2$ dehalogenation or by $(RP)_5$ pyrolysis can be either traced mass sepctroscopically or trapped e.g. with disulfides or α,β-diketones:[32]

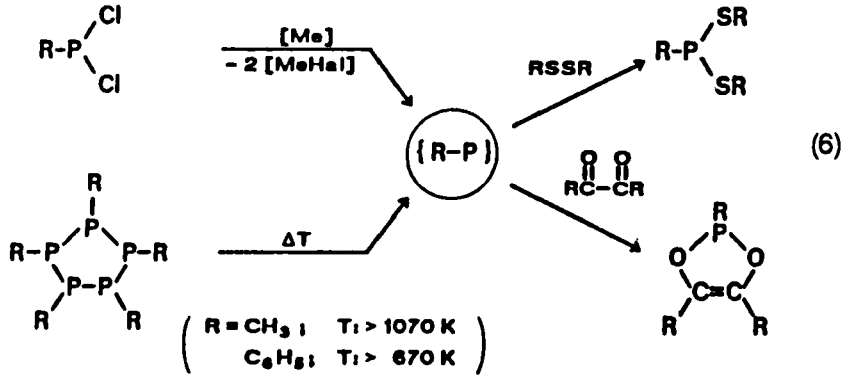

According to ab initio calculations,[33] the triplet ground state $^3(H_3C\text{-}P)$ is expected to be stabilized by 138 kJ/mol relative to the excited singlet state $^1(H_3C\text{-}P)$.

In an attempt to generate the still unknown $H_3C\text{-}P{=}P\text{-}CH_3$ under nearly unimolecular gasphase conditions, we have passed a stream of $H_3C\text{-}PCl_2$ over Mg powder under PE-spectroscopic real-time gas analysis.[19,23] The reaction takes place in the rather narrow temperature range between 570 K and 620 K and yields a product mixture (Figure 10), from which by fractionation using the intense cooling traps fitted with bypasses (cf. Figure 5) the compounds $P(CH_3)_3$, CH_4, $(H_3C)_2P\text{-}P(CH_3)_2$ and $(PCH_3)_5$ can be isolated and identified either by their PES ionization or mass fragmentation patterns (Figure 10). The product distribution suggests an intermediate formation of chemisorbed phosphinidenes at the Mg metal surface:

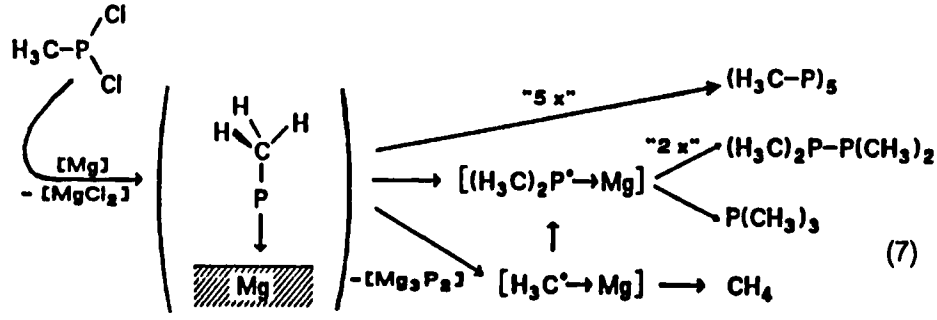

(7)

The driving force is the thermodynamically favorable formation of $[MgCl_2]$. The presumably low activation barrier for (H_3CP) surface migration should allow oligomerisation e.g. to the isolated and spectroscopically characterized pentamer $(H_3C\text{-}P)_5$. The dissociation of $[H_3CP \rightarrow Mg]$ to a surface phosphide $[Mg_3P_2]$ and chemisorbed methyl radicals $[H_3C^{\bullet} \rightarrow Mg]$ as indicated by the considerable amount of CH_4 observed, would be consistent with mechanistic studies for alkyl Grignard RMgHal formation[34] as well as with ultrahigh vacuum investigation results for the reaction of H_3CBr at Mg [001] surfaces.[35] It also would explain via radical alkylation of $[H_3CP \rightarrow Mg]$ to $[(H_3C)_2P^{\bullet} \rightarrow Mg]$ and $[(H_3C)_3P \rightarrow Mg]$ how both $P(CH_3)_3$ and the dimer $(H_3C)_2P\text{-}P(CH_3)_2$ are formed as unequivocally identified products (Figure 10) in the heterogeneous reaction of $H_3C\text{-}PCl_2$ at magnesium powder.

The product mixture obtained analogously from ethyldichlorophosphane at 150 K higher temperature

$$H_3C\text{-}H_2C\text{-}PCl_2 \xrightarrow[>720\,K]{[Mg]} \left\{ \begin{array}{l} H_3C\text{-}H_2C\text{-}PH_2 + (H_3C\text{-}H_2C)_2PH + (H_3C\text{-}H_2C)_3P \\ + (H_3C\text{-}H_2C\text{-}P)_5 + P_4 \\ + H_2C{=}CH_2 + H_3C\text{-}CH_3 + H_3C\text{-}H_2C\text{-}CH_2\text{-}CH_3 \end{array} \right. \quad (8)$$

adds the following: the detection of n-butane as a $H_3C\text{-}H_2C^{\cdot}$-dimer confirms the likely presence of [$H_3C\text{-}H_2C^{\bullet} \rightarrow Mg$] as a source also for $H_3C\text{-}CH_3$ and $H_2C{=}CH_2$. The latter indicates [$HP \rightarrow Mg$] as chemisorbed species, which in turn allows to rationalize the formation of $H_3C\text{-}H_2C\text{-}PH_2$, $(H_3C\text{-}H_2C)_2PH$ and also of P_4. Again the oligomer $(H_3C\text{-}H_2C\text{-}P)_5$ can be isolated and identified mass spectroscopically (Figure 10).

Iso(valence)electronic nitrenes on metal surfaces [RN -- Me] can be generated more elegantly by catalytic split-off of thermodynamically favorable leaving groups like N_2 from alkyl azides $RN\text{-}N_2$[36] or CO from alkyl isocyanates RN-CO.[37] Depending on their alkyl substituents and the respective metal surface, various secondary reactions lead to chemidesorbed products such as $[(H_3C)_2HCN \rightarrow Ni] \rightarrow CH_4 + H_3CCN$[37] or $[(H_3C)_3CN \rightarrow Ni] \rightarrow (H_3C)_2C{=}CH_2 + NH_3 + N_2$[37] i.e. presumably involving a surface nitrene [HN → Ni], which disproportionates into NH_3 and N_2. Therefore, the above assumptions for (8), i.e. formation of [$H_3CH_2CP \rightarrow Mg$], its ethen elimination to [$HP \rightarrow Mg$] and the disproportionation to elemental P_4, at least do have a close analogy and it is hoped that our results will stimulate further research in surface phosphinidenes.

4. GASPHASE PREPARATION OF UNSATURATED OXY- AND THIOPHOSPHORUS CHLORIDES

4.1. Cl-P=O and Cl-P=S: Gas/Surface Reactions at Silver Wool

The title molecules[15,38] each contain 18 valence electrons and, therefore, are iso(valence)electronic with compounds exhibiting bent structures such as ONCl, OSO, OOO, FCF, and NSF - as predicted by the well-known Walsh rules.[39] They are also of interest as prototype molecules of novel saturated phosphorus compounds such as the diphosphenes R-P=P-R,[30,31] in which phosphorus of coordination number 2 is kinetically stabilized by bulky substituents.

Both Cl-P=O and Cl-P=S can be prepared in the gasphase by dechlorination of the corresponding trichlorides with silver turnings above 1100 K:[15,38]

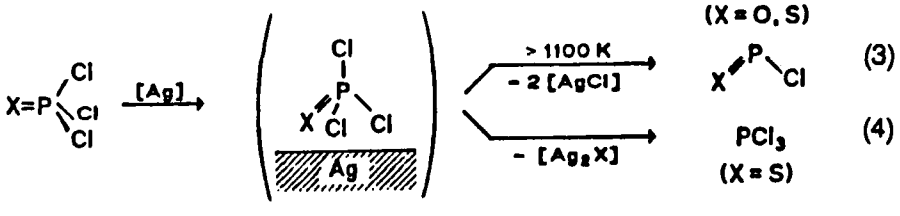

and their structures elucidated by IR spectroscopy after isolation in an argon matrix at 15 K.[38] The PE spectroscopic ionization patterns (Figure 11) not only allow to optimize the reaction conditions, but yield additional information via their

assignments based on ab initio SCF calculations.[15] The following details shall be emphasized:

- ▷ The dehalogenation of oxide chlorides by Ag is due to the thermal instability of Ag_2O above 570 K; via this route, numerous other molecules containing central atoms of low coordination number can be prepared.[38]
- ▷ As concerns the PE spectroscopic optimization of the S=P-Cl preparation, selected for illustration (Figure 11), at 1150 K the ionization pattern of the starting material S=PCl_3 has disappeared completely (Figure 11:⇨). The resulting S=P-Cl is contaminated by PCl_3 as a surface reaction side product (4); its ionization bands can be eliminated by computer subtraction (Figure 11: ---->) of its prerecorded and stored PE spectrum.
- ▷ The He(I)PE spectra of O=P-Cl and S=P-Cl (Figure 11) each display six ionization bands, which can be unequivocally assigned via Koopmans' correlation, $IE_n^v = -\varepsilon_j^{SCF}$, with ab initio SCF eigenvalues.
- ▷ Comparison of each the corresponding radical cation states (Figure 11: dotted connecting lines) shows that the smaller effective nuclear charge of the sulfur atom causes a lowering of all ionization energies by approximately 1 eV.

The ab initio calculations, in which relatively large basis sets (e.g. for the second row elements 11s, 7p, 1d[15]) have been employed, yield the following additional information:

- ▷ The structural data of S=P-Cl and O=P-Cl calculated for the respective minima of the total energies (Figure 10) differ only slightly from those of the educts S=PCl_3 and O=PCl_3: the influence of the electron pair at the P atom generated by chlorine split-off is manifested by contraction of the O=P-Cl angle from 115°C to 109°C and by that of the S=P-Cl angle from 116°C to 110°C. According to the calculations, the P=O and P=S bond lengths are 1 - 2 pm shorter and the PCl distances 6 pm longer than in the corresponding trichlorides.
- ▷ The radical cation ground states $\tilde{X}(^2A')$ of both molecules can be characterized from the MO contour-line diagrams shown here for the oxygen derivative

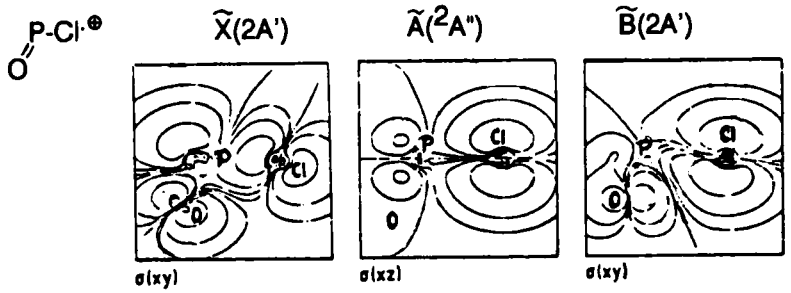

(9)

as electron pair ionizations with a major P-contribution. In both cases, a π state $\tilde{A}(^2A'')$ follows, with predominant Cl-contribution in O=P-Cl and a

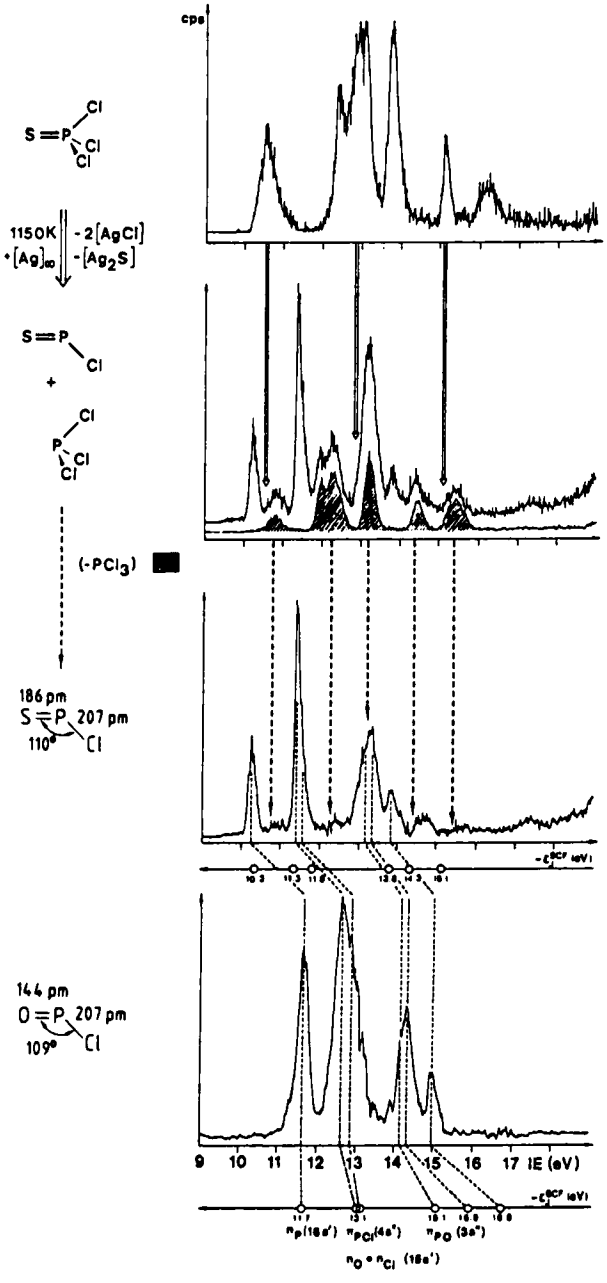

FIGURE 11. He(I)PE spectra between 9 and 19 eV of $SPCl_3$ at 300 K and of the product mixture S=P-Cl + PCl_3 resulting from the reaction with silver at 1150 K. The PE spectrum of S=P-Cl is obtained by computer-subtraction (---->) of the PCl_3 ionization bands[33] (hatched) and assigned by $M^{\cdot\oplus}$ state comparison with $O{=}P{-}Cl^{\cdot\oplus}$ as well as by Koopmans' correlation with ab initio SCF eigenvalues. The structural data listed for S=P-Cl and O=P-Cl are those calculated for the minima of total energy.

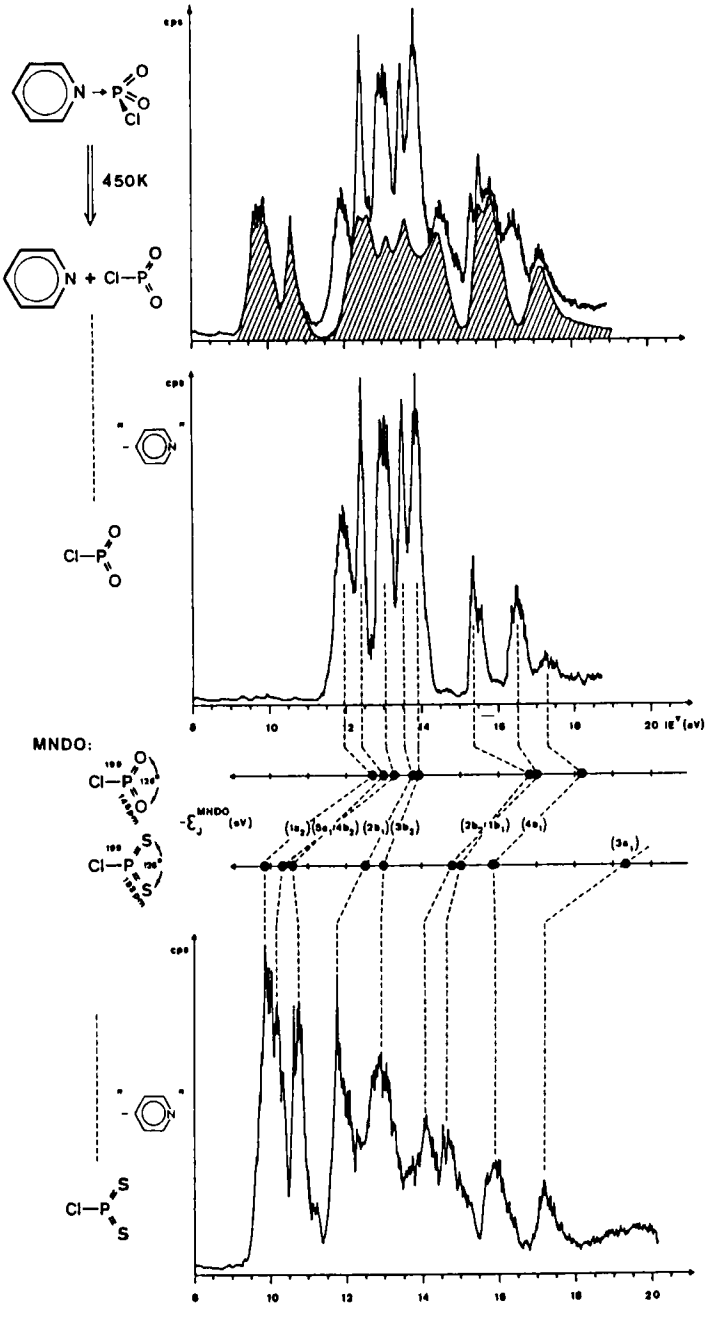

FIGURE 12. He(I)PE spectra of the phosphoric acid chloride pyridinium betaine dissociation at 450 K into Cl-P(=O)$_2$ and pyridine (hatched), the digital subtraction of which yields those of both dioxo and dithio phosphorus (V) chlorides.[16] Their assignment via Koopmans correlation, $IE_n^v = -\varepsilon_j^{MNDO}$, is based on geometry-optimized MNDO calculations[16] with the resulting minimum total energy structures also shown.

rather large S contribution in Cl-P=S. Expectedly, for the second π states C(^{2}A'') (Figure 11: 13.3 and 14.3 eV), these relations are inverted. The third $M^{\cdot\oplus}$ states B(^{2}A') in between correspond within the MO picture to the antibonding combinations of the electron pairs n_{Cl} - n_O and n_S - n_{Cl}. At higher energies, the radical cation states of A' symmetry are characterized by a larger contribution of σ-bonding electrons.

Summarizing, both molecules Cl-P=O and Cl-P=S are thermodynamically stable and do not exhibit any unusual structural features. These parent molecules, which readily form on silver surfaces by chlorine abstraction, are short-lived only due to their rapid oligomerization and thus have to be prepared under nearly unimolecular conditions, i.e. in a gas flow under reduced pressure. If, however, the kinetic instability could be overcome by excessive steric shielding from bulky substituent groups, bottable derivatives might be feasible.

4.2. Cl-P(=O)$_2$ and Cl-P(=S)$_2$: Gasphase Dissociation of Pyridinium Betaines

Four-atom chalcogen element halides, $Hal_2E{=}X$ and $Hal{-}E(=X)_2$, containing 24 valence electrons are planar according to 'classical' Walsh rules[39] and for main group elements E located between the iso(valence)electronic molecules F_3B and SO_3. Despite of their fundamental importance concerning π/σ bonding models, so far only the (diamagnetic) neutral compounds $Hal_2C{=}O$ (Hal = F,Cl,Br),[40] $Hal_2C{=}S$ (Hal = F,Cl),[40] $F_2C{=}Se$[41] as well as $HalN(=O)_2$ (Hal = F,Cl)[40] have been characterized by their ionization patterns, because readily oligomerizing derivatives like Cl-P(=O)$_2$ could only be generated by oxidation of Cl-P=O[15] and investigated subsequently in low temperature Ar matrices.[42] There is, however, a more elegant and convenient access to both Cl-P(=O)$_2$ and the still unknown Cl-P(=S)$_2$ by starting from the easily prepared pyridinium betaines:[43]

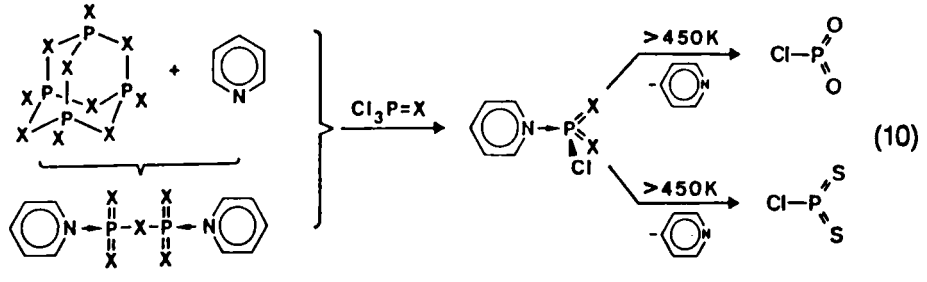

According to the recorded PE spectra (Figure 12), evaporation at 10 Pa pressure immediately yields mixtures of pyridine and each Cl-P(=O)$_2$ or Cl-P(=S)$_2$, the ionization patterns of which may be 'extracted' by digital subtraction of the prerecorded H_5C_5N spectrum (Figure 12: hatched).

The geometry-optimized MNDO calculations used for the spectroscopic assignment (Figure 12) via Koopmans' theorem, $IE_n^v = -\varepsilon_j^{MNDO}$, also provide information on structures and charge distributions of Cl-P(=O)$_2$ and Cl-P(=S)$_2$ and thus allow a molecular state comparison (Figure 4) with other 4 atom/24 valence electron planar compounds like Cl_3B, $Cl_2C{=}S$, Cl-N(=O)$_2$ and SO_3 (Figure 13). From the resulting M and $(\pi)M^{\cdot\oplus}$ correlation diagrams, inter alia, the following similarities or differences become apparent:

- ▷ The structures of the 6 individual molecules are largely comparable, if the different covalent radii r_E and r_X[44] are taken into account.
- ▷ All of them possess each 6 π electrons, giving rise to π radical cation states of either $1e'' < 1a_2''$ (D_{3h} symmetry) or $1a_2 < 2b_1 < 1b_1$ (C_{2v} symmetry; except $Cl_2C{=}S$ (···) with its rather low $\pi_{C=S}$ ionization. Correlation according to dominant $(\pi)M^{\cdot\oplus}$ contributions readily demonstrates the effect of varying effective nuclear charges: thus $\pi_b(1b_1)$ is lowered on exchange S → O and P → N from 14.5 eV to 18.1 eV(!). From the $M^{\cdot\oplus}$ ($1a_2$) states exhibiting nodal planes through their Cl-E bonds, concomitantly, the parameters α_S = 9.8 eV as well as α_O = 12 eV can be read off.
- ▷ The overlapping π interactions can be rationalized by second order perturbation, $\beta^2_{Cl/PX2}/\Delta\alpha_{Cl/PX2}$: the accompanying MNDO calculations predict for Cl-P(=S)$_2$ in its $\pi(2b_1)$ and $\pi(1b_1)$ states each 50 % Cl- and PS_2-contributions, whereas for Cl-P(=O)$_2$ in $\pi(2b_1)$ 85 % Cl- and vice versa - in $\pi(1b_1)$ 88 % PO_2- contributions are suggested. As concerns Cl-N(=O)$_2$, 95 % Cl result for $\pi(2b_1)$ and 94 % NO_2 for $\pi(1b_1)$.
- ▷ The MNDO charge distributions also reflect the π ionization patterns: except for the thio derivative $Cl_2C{=}S$, the positively charged E centers (Figure 12: Q_μ^{MNDO}) are surrounded by negative ligands X, which back-donate considerable π electron densities (Figure 13: $q_{\mu,\pi}^{MNDO}$). This is best exemplified by Cl_3B, which in contrast to diborane $(H_3B)_2$, therefore, remains monomeric.
- ▷ Within the general comparability of the 4 atom/24 valence electron molecules displayed in Figure 13, the following polarization trends are observed: $\overleftarrow{B\text{-}Cl} > \overrightarrow{C\text{-}S}$ or $\overrightarrow{P\text{-}S} < \overrightarrow{P\text{-}O} < \overrightarrow{N\text{-}O} << \overrightarrow{S\text{-}O}$. Especially the extreme π back donation in SO_3, the S center of which according to the MNDO calculation bears a +1.6 charge, and which contributes formally 3 of the 6 π electrons, compensates for the sulfur electron deficit within the σ skeleton.

The preceding discussion of the Cl-P(=O)$_2$ and Cl-P(=S)$_2$ ionization patterns based on MNDO total energy minima structures, eigenfunctions and the resulting total as well as π electron densities resulting from them, has numerous implications. To just mention the most obvious one, due to their rather low first ionization energies and their favorable charge distribution, derivatives R-P(=S)$_2$ should be well-suited metal complex ligands. Within this context, therefore, the gasphase preparation of H_3C-P(=S)$_2$ and H_5C_2P(=S)$_2$ from their stable dimers shall be emphasized:[45]

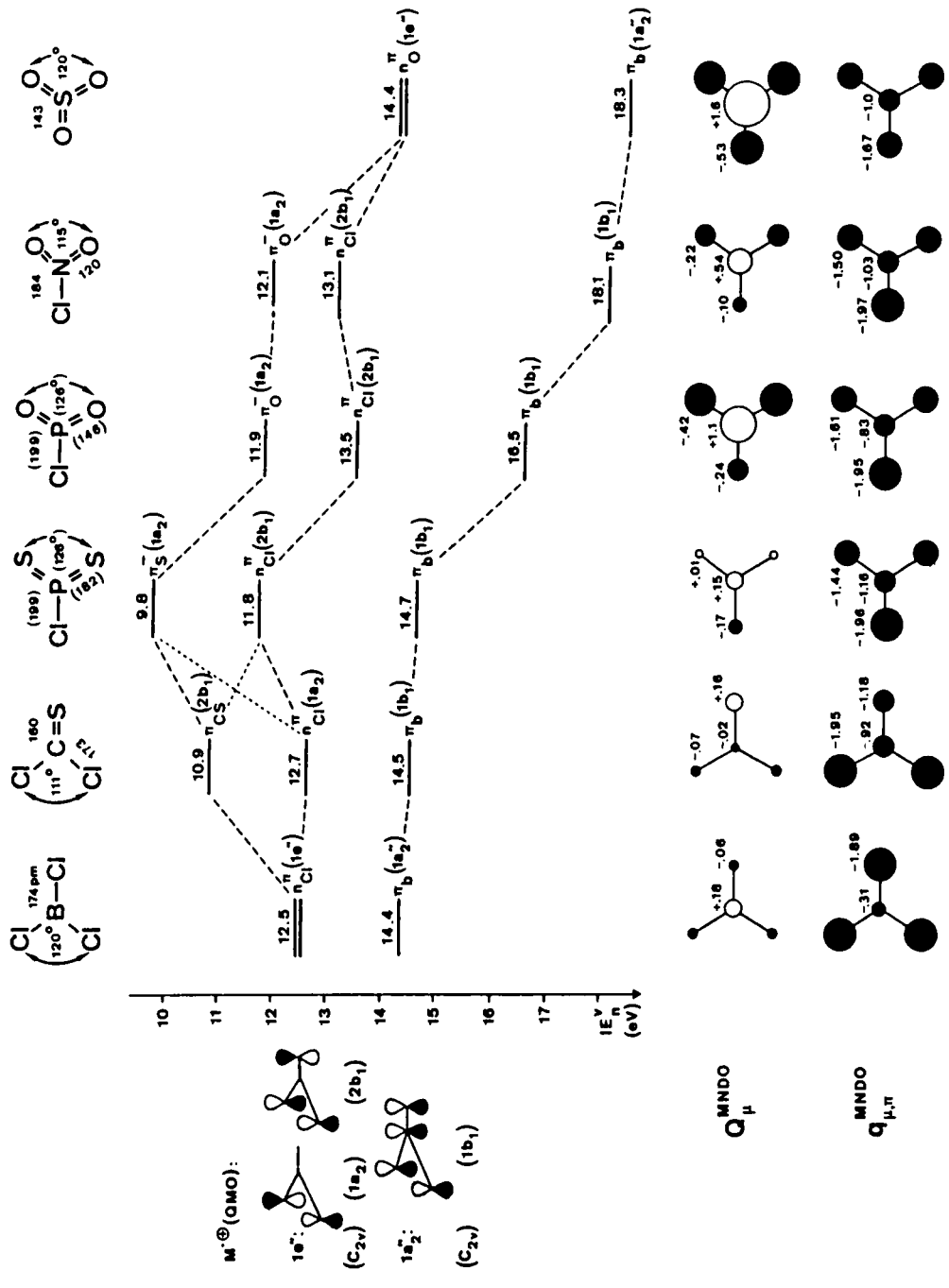

FIGURE 13. Experimental[44] or calculated[16] structures of Cl_3B, $Cl_2C{=}S$, $Cl\text{-}P(=S)_2$, $Cl\text{-}P(=O)_2$, $Cl\text{-}N(=O)_2$ and SO_3, their vertical π ionization energies with $M^{\cdot\oplus}$ state assignment as well as their total and π charge densities from geometry-optimized MNDO calculations (see text).

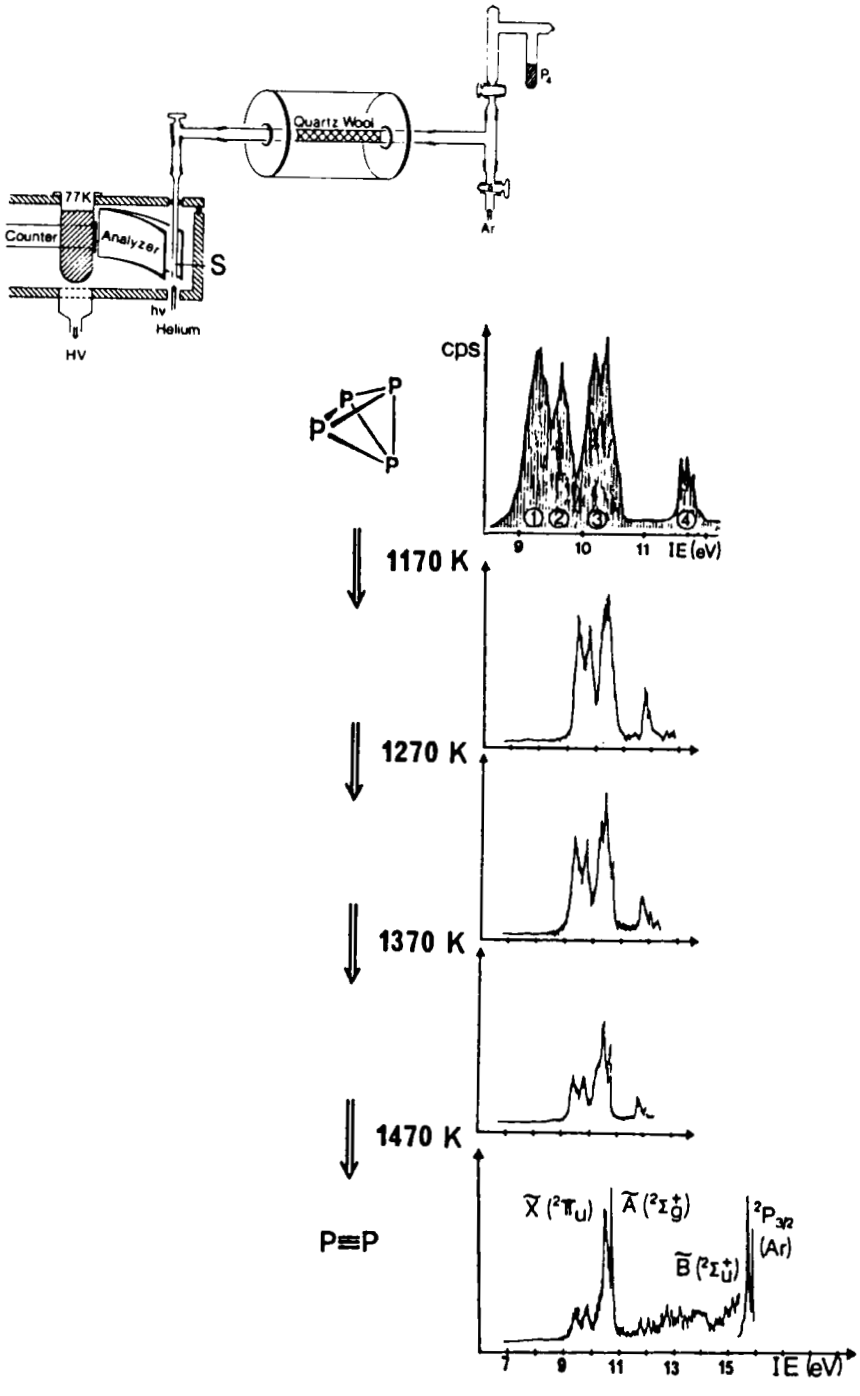

FIGURE 14. He(I)PE spectra of phosphorus vapor at 298, 1170, 1270, 1370, and 1470 K, calibrated with the $^2P_{3/2}$ (Ar) band at 15.76 eV (for the P_2 radical cation state assignment see text).

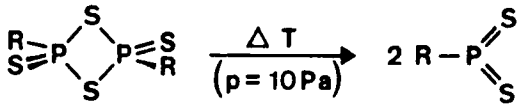

(11)

Altogether, the numerous compounds R-P(=X)$_2$ known containing a threefold coordinated P(V) center and stretching from $(R_3Si)_2N$-P(=NSiR_3)$_2$ to [$R_4As^{\oplus}$][$PS_3^{\ominus}$],[30] still can be complemented with unknown ones - among them the 24 valence electron containing parent molecules Cl-P(=S)$_2$ or H_3C-P(=S)$_2$, which provide so valuable information on their molecular states (Figure 13).

5. THE GASPHASE EQUILIBRIUM $P_4 \rightleftarrows 2\,P_2$ VISUALIZED

5.1. PE Spectroscopic Determination of the Equilibrium Constant

In the gas phase, the P_4 tetrahedron decomposes at temperatures above 1100 K into two P_2 fragments:[46]

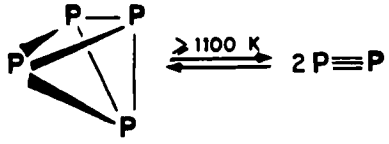

(12)

The dissociation energy, D_0 = 217 kJ/mol,[47] is used to produce the then stable diatomic species P_2, iso(valence)-electronic to the nitrogen molecule, by formally breaking four PP bonds while two are shortened from 221 pm[48] to 189 pm[47].

Both element modifications have been investigated repeatedly by photoelectron spectroscopy,[2,14,23,48,49] and the observed ionization patterns (Figure 14) are assigned to the radical cation state sequence $^2E < {}^2T_2 < {}^2A_1 < {}^2T_2 < {}^2A_1$ for P_4 and $^2\Pi_u < {}^2\Sigma_g^+ < {}^2\Sigma_u^+$ ... for P_2. The P_4 and P_2 PE spectra recorded suggest - assuming comparable ionization cross sections - that the concentration of the individual components may be determined simultaneously in their gaseous mixtures (Figure 14). Considering in addition the PE spectrometer design i.e. a flow system at reduced pressure in a helium atmosphere, it seemed feasible to measure the temperature dependence of the equilibrium (13) by means of the advantageous PE spectroscopic real-time gas analysis[23] using only millimole quantities of white phosphorus, a dangerous vapor at higher temperatures, within a single day.

For the PE spectroscopic measurement, the dry white phosphorus is distilled through CaH_2 in a glass apparatus that had been browned by coating with silver mordant and consecutive tempering at 700 K.[14] The P_4 storage trap

as well as an argon-carrier gas inlet are both connected to the pyrolysis tube filled with quartz wool to improve heat transfer from the temperature-controlled furnace (Figure 14). The P_4/P_2 molecule beam from the heating zone and the photons from an open helium discharge meet in the target chamber of the PE spectrometer in front of the slit (Figure 14: S), through which the emitted electrons pass via the analyzer into the counter. Essential for reliable measurements are a distance, as short as possible, between heating zone and target chamber as well as an effective thermal insulation of the connecting tube. After recording a PE spectrum of P_4 at 300 K, the furnace temperature was raised in steps of 100 K. For the evaluation of the temperature-dependent P_4 : P_2 ratios, the planimetrically determined and normalized band intensity ratios, $I_3(P_4)/I_3$ and $2\ I_3(P_2)/I_3$, are used, which are proportional to the partial pressures and yield - via the dissociation coefficient α - the dissociation constant K_P at various temperatures (pressure P = 0.28 torr; for details cf.[14]):

$$p(P_4) = [(1 - \alpha)/(1 + \alpha)]P$$

$$p(P_2) = [2\alpha/(1 + \alpha)]P$$

$$K_P = p^2(P_2)/p(P_4) = [4\alpha^2/(1 - \alpha^2)]P \qquad (13)$$

T, K	α	K_P	$\ln K_P$
1170	0.1	1.49×10^{-5}	−11.11
1270	0.3	1.57×10^{-4}	−8.76
1370	0.5	6.07×10^{-4}	−7.41
1470	0.8	2.02×10^{-3}	−6.20

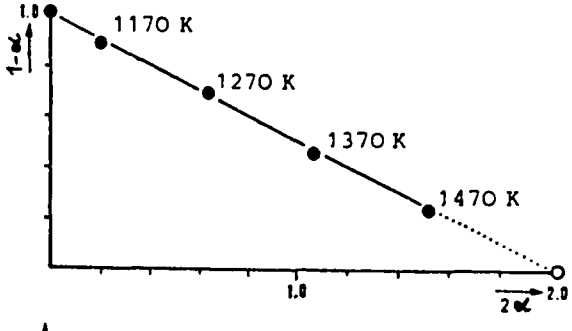

(14)

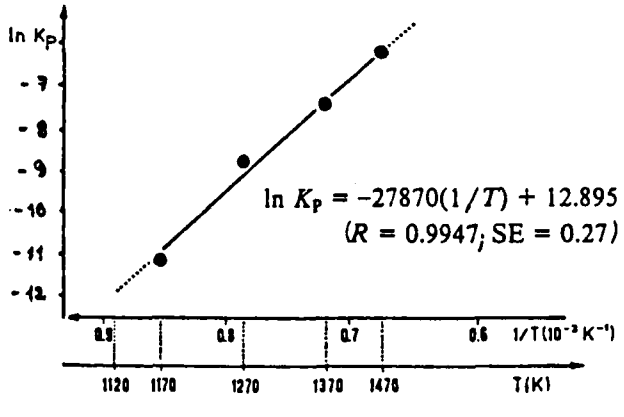

(15)

Altogether, from the decreasing intensities of the first two PE bands and the increasing one of the third band system (Figure 14) - also indicating that no other species is present in the thermal P_4 fragmentation -, both the correlations of the residual (1 - α) P_4 molecules vs. the (2α) P_2 fragments formed within the equilibrium (13) as well as of ln Kp vs. the reciprocal temperature result in straight regression lines. If, in addition, the temperature dependence of ln K_p (15), which agrees with results from other measurement techniques,[46] is inserted into the thermodynamic relation, ln $K_p = \Delta H/RT + \Delta S/R$, approximate values for the dissociation enthalpy, $\Delta H \sim 232$ kJ/mol, and the associated entropy difference $\Delta S \sim 107$ J/mol K are obtained, of which ΔH corresponds to the literature value of the P_4 dissociation energy, $D_0 = 217$ kJ/mol.[47]

As a useful advice for the destruction of white phosphorus residues, which can be quite dangerous especially when spread out, bathing of all used glassware in an aqueous sodium hypobromite (NaOH + Br_2) solution is recommended.[14]

5.2. Approximate Energy Hypersurface Calculation

MNDO calculations[50] for P_4 and P_2 based on their structural parameters (P_4:[46] d_{PP} = 221 + 2 pm; $\sphericalangle$(PPP) = 60° and P_2:[47] d_{PP} = 189 pm) or by using the Fletcher/Davidson/Powell geometry optimization subroutine, allow, via Koopmans' theorem, $IE_n^v = -\varepsilon_n^{MNDO}$, to reproduce satisfactorily their PE spectroscopic ionization patterns (Figure 14). Therefore, we attempted to speculate about the P_4 cluster opening (Figure 14), which could occur in several ways by opening one to four PP edges:

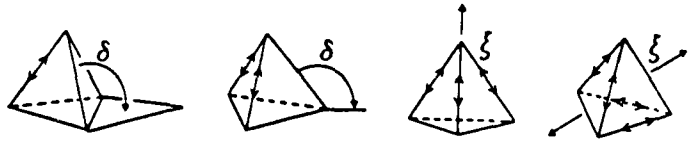

(16)

ΔPP 1 2 3 4

So far, only the dissociation by simultaneously breaking Δ(PP) = 4 bonds has been considered in the literature.[51] The analogous though fictious dimerization of nitrogen $2N_2 \rightleftarrows N_4$ has been rationalized using qualitative orbital diagrams within the framework of the Woodward-Hoffmann rules:[52] accordingly, the reaction is forbidden in D_{2d} as well as skew-D_2 symmetry due to a $b_1 \times b_2$ crossing. Based on the experimentally supported applicability of MNDO for P_4 and P_2 e.g. by correctly reproducing all structural parameters,[14] we have screened all possibilities (16) in tentative caclulations by varying the respective angles δ or the reaction coordinate ξ as follows:

ΔPP = 1: The length of the opening bond is increased in steps of Δd_{PP} = 20 pm up to 381 pm, while all others are kept fixed.

ΔPP = 2: The angle δ is reduced to 0^{o} by 15^{o} increments, thereby increasing the distance along the opening bonds up to 420 pm.

ΔPP = 3: Steps of $\Delta\xi$ = 30 pm between 180 and 380 pm from the basal triangle have been considered, elongating the bonds involved up to 400 pm.

ΔPP = 4: Among the possibilities, twisting of the dihedral angle by increments $\Delta\omega = 11^{o}$ in the direction toward a planar P_4 skeleton as well as increasing the distance between the two P_2 subunits along the C_2 axis by steps $\Delta\xi$ = 30 pm has been tested.

Of all the possibilities (16) considered, the dissociation by breaking ΔPP = 4 bonds simultaneously yielded the smallest increase in MNDO total energy. Obviously, this movement within the 3 · 4 - 6 = 6-dimensional P_4 hyperspace must occur along and between some deeper troughs and has to cross only one of the relatively lower saddles in total energy. Therefore, an additional variation of the P_4 tetrahedral bond lengths has been carried out, and all the results were combined to plot the approximate energy hypersurface, which is presented in Figure 15.

The barrier for the crossover between the two troughs holding the stable molecules P_4 and P_2 has been calculated without configuration interaction and amounts to E_{total}^{MNDO} ~ 177 kJ/mol. Although some 40 kJ/mol below the experimental value of D_0 = 217 kJ/mol, the MNDO result - presumably due to its reliable phosphorus parametrization - is one of the numerically closest reported so far for the $P_4 \rightleftarrows 2P_2$ equilibrium.[53] As a rationale, the simultaneous opening of four bonds and shortening of two bonds - even exaggerated by the MNDO procedure down to a shallow minimum at about 160 pm - might be considered. Contrary to [51] and as required by the symmetry forbiddeness quoted,[52] the orbital crossing $b_1 \times b_2$ is observed. In addition, the individual pathways (16) as explored by our semiempirical MNDO calculations can be discussed within the orbital correspondence analysis in maximum symmetry[54] as follows: The four pathways (16) can be labeled e for ΔPP = 1 and 2, e or b_2 (depending on the axis chosen) for ΔPP = 3, and a_1 for ΔPP = 4. The forbidding crossing $b_1 \times b_2$ can be avoided, in principle, by an a_2 ($=b_1 \cdot b_2$) displacement, i.e. within the D_{2d} subgroup S_4. Unfortunately, however, among the six vibrational modes of P_4 in D_{2d} symmetry, which transform as $2a_1 + b_1 + b_2 + e$, there is no internal coordinate of the irreducible representation a_2 except for the rotation R_z. In second order, the only potentially useful displacement ($b_1 + b_2$) that retains some symmetry at all would reduce D_{2d} to C_2 and should be considered more explicitely in future elaborations on the $P_4 \rightleftarrows 2P_2$ equilibrium.

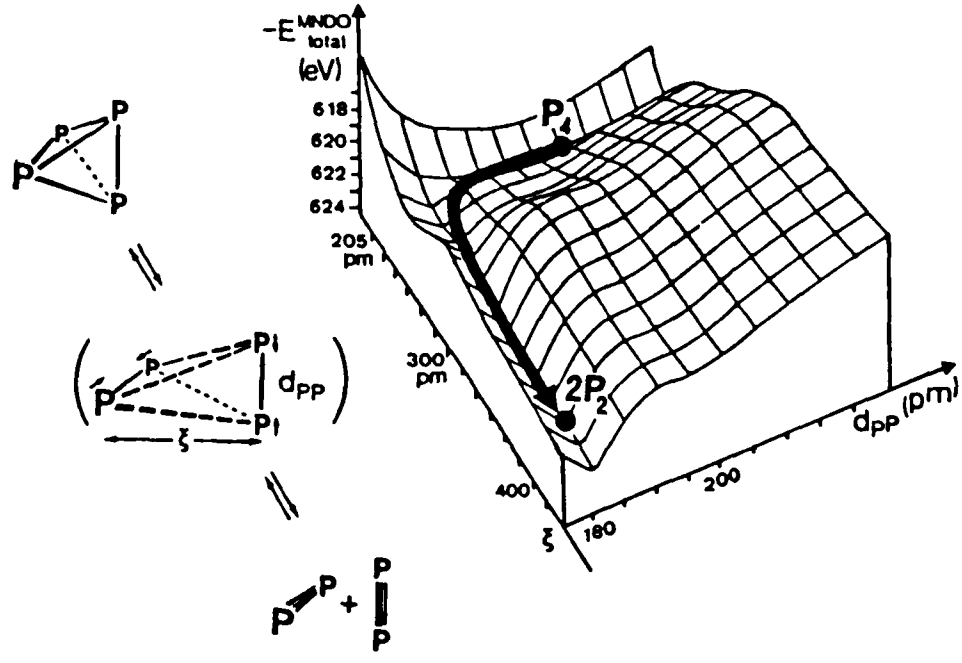

FIGURE 15. Section of a MNDO hypersurface generated by selecting from the $3 \cdot 4 - 6 = 6$ degrees of freedom of the P_4 ensemble the dissociation coordinate ξ and the distance d_{PP} of the perpendicular PP bonds, while simultaneously optimizing all others by the Fletcher/Davidson/Powell subroutine of the MNDO program (see text).

In summary, the MNDO hypersurface (Figure 15) displaying deep troughs for P_4 and P_2 provides another supporting argument for why on heating of white phosphorus up to 1470 K no other phosphorus species such as P atoms or thermodynamically presumably more favorable molecules such as P_6 or P_8[54] could be detected PE spectroscopically.

6. THERMOLYSIS REACTIONS YIELDING 2-PHOSPHAPROPENE $H_3C\text{-}P{=}CH_2$

6.1. Thermal HCl Elimination from Dimethylchlorophosphane

The report on investigations of thermal or heterogeneously catalyzed dehydrohalogenations of various phosphorus compounds by the Frankfurt PES and ESR/ENDOR group (chapter 1.3), so far has covered alkyldichlorophosphanes $RPCl_2$, which have been pyrolyzed (chapter 2.2), reacted with the catalyst [10 % $MgCl_2$-MgO/SiO_2] (chapter 2.2) or with Mg metal (chapter 3). As a represen-

tative example of numerous dialkylchlorophosphanes R_2PCl_2 also investigated,[22] the 'parent' dimethyl derivative $(H_3C)_2PCl$ is selected.[17]

A large number of X-P=Y compounds containing[18] valence electrons and phosphorus of coordination number 2 have been synthesized, e.g. Cl-P=O and Cl-P=S[15,38] (cf. chapter 4.1), H_3C-P=S,[55], Cl-P=CH_2[56] and, more recently, H_3C-HC=PH.[26] All are bent, as predicted by the Walsh rules,[39] and may be regarded as propene analogues within the 'united atom' approximation.[3,4] The novel molecule 2-phosphapropene can be prepared from chlorodimethylphosphane by gasphase pyrolysis and identified by its photoelectron (PE) and mass spectra (Figure 16):[17]

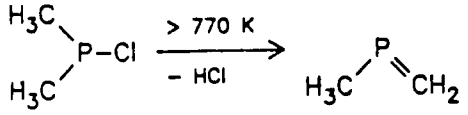

(17)

According to the useful electron counting rule of thumb[2,5] (Σ np_E + Σ $1s_H$)/2 = n IE^V, 6 ionization bands are expected in the He(I)PES measurement region for a molecule of composition C_2H_5P, i.e. containing seven $np_{Element}$ and five $1s_H$ valence electrons. All of them are indeed observed each for the isomers 2-phosphapropene[17] (Figure 16), phosphirane $(H_2C)_2PH$[58] as well as 1-phosphapropene.[26] As concerns the first band in the PE spectrum of 2-phosphapropene (Figure 16), it comprises two ionizations, which according to the accompanying MNDO calculations, generate the radical ground state $\tilde{X}(^2A'')$ with predominant $\pi_{P=C}$ bond contribution and its first excited state $\tilde{A}(^2A')$ of P lone pair character n_P. The following 4 ionizations between 12 eV and 16 eV are asigned to the σ molecular skeleton in the sequence $\sigma_{HCPCH}(a') < \pi_{CH3}(a'') < \sigma_{CH3}(a') < \sigma_{CH2}(a')$. The additional weak-intensity band at 17.0 eV, according to the MNDO calculation (Figure 16) results from ionization into a radical cation state with large phosphorus 3s contribution.

6.2. Thermal Dehydration of Dimethylphosphane Oxide

A variety of unsaturated organophosphorus compounds containing structural units like -C≡P, >C=P-, -P=C=P-, -C≡P< or -C-P< and a manifold of substituents have been synthesized in recent years via numerous different routes.[30,31,59] Unknown, however, is their preparation by thermal dehydration,[60] for example of dialkylphosphane oxides, $R_2HP{=}O$, which are now being produced on a large scale.[61] In general, the P=O bond, exhibiting bond dissociation enthalpies of 520 to 270 kJ/mol,[62,63] is regarded as being highly favored energetically and its preferential formation exploited in the Wittig and Arbusov reactions.

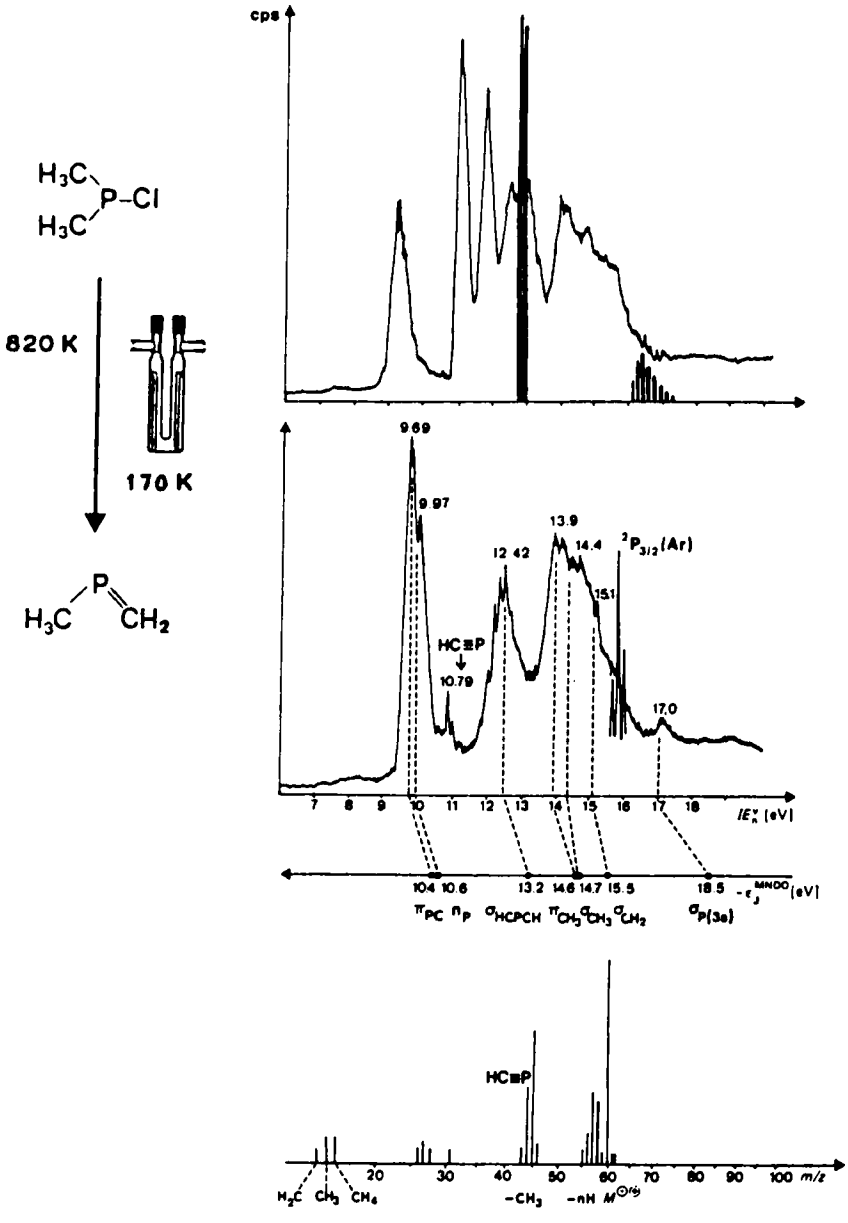

FIGURE 16. He(I)PE spectra of $(H_3C)_2PCl$, which contains traces of HCl (black), and of its pyrolysis product $H_3C\text{-}P{=}CH_2$ at 820 K, assigned via Koopmans'correlation, $IE_n^v = -\varepsilon_j^{MNDO}$, with MNDO eigenvalues. Excess starting material and the cleavage product HCl are removed by condensation in a 170 K intense cooling trap (cf. Figure 5). Under the PE spectroscopically optimized pyrolysis conditions, in addition a mass spectrum has been recorded, which also confirms the presence of $HC{\equiv}P$, presumably formed by CH_4 elimination, $H_3C\text{-}P{=}CH_2 \rightarrow CH_4 + HC{\equiv}P$, at higher temperature.

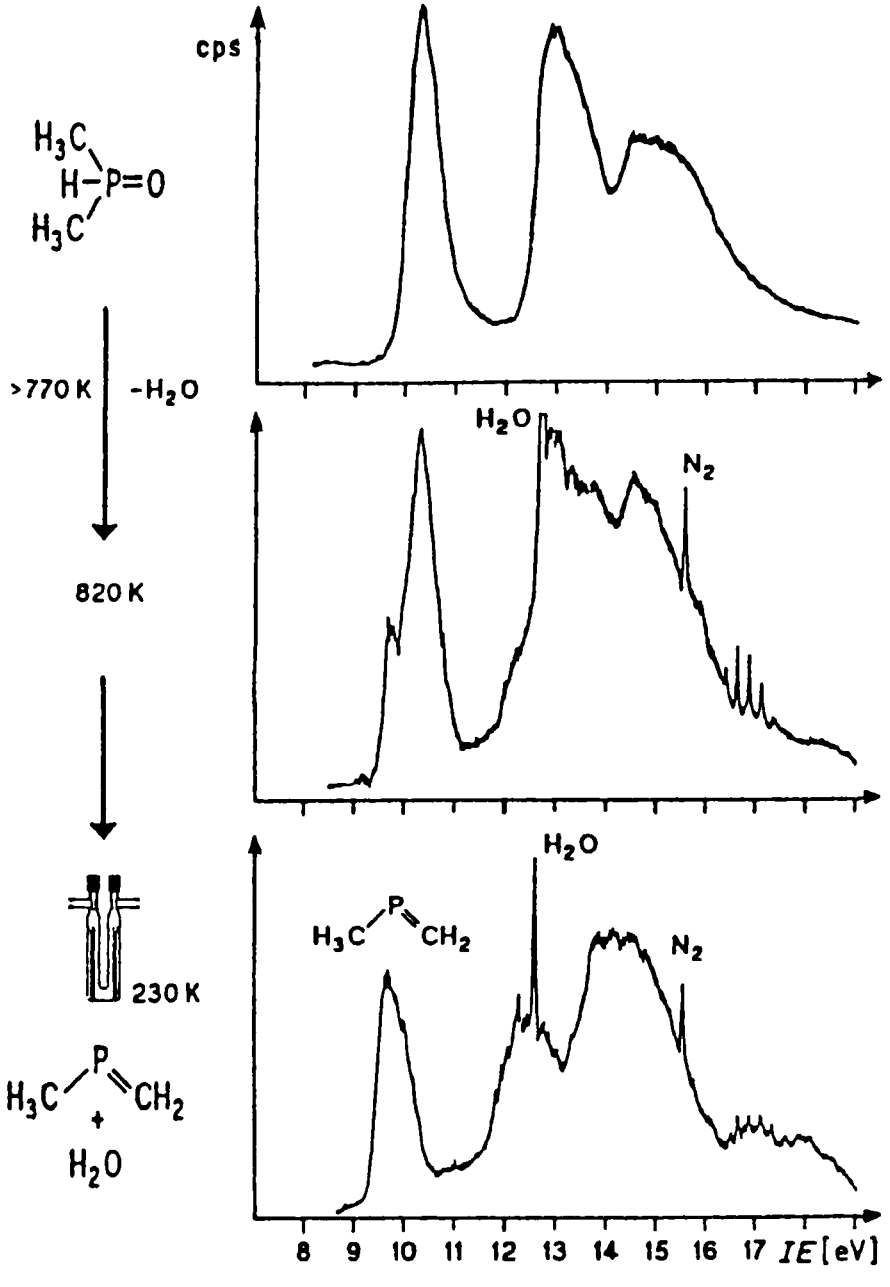

FIGURE 17. He(I)PE spectra of dimethylphosphane oxide and its thermal fragmentation mixture after passing a horizontal quartz tube (Figure 5) filled with quartz wool and heated to 820 K as well as of $H_3C\text{-}P{=}CH_2$ (Figure 16) and H_2O after removing undecomposed $(H_3C)_2HP{=}O$ in a 230 K cold trap (calibration by $\tilde{X}\,(^2\Sigma_g)$ of N_2 at 15.60 eV).

For the first time, a selective H_2O elimination is observed in the gas-phase thermolysis of dimethylphosphane oxide[18,22] to give 2-phosphapropene (Figure 17), which has already been generated by HCl elimination from dimethylchlorophosphane[17] (Figure 16):

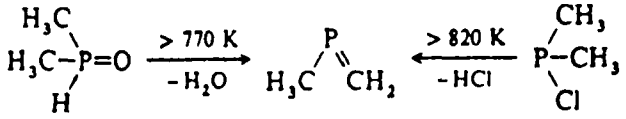

(18)

When the decomposition of $(H_3C)_2HP=O$ on quartz wool is monitored by PE spectroscopic real-time analysis[23] (chapter 2.1), a method that has proved especially valuable for studying reactive molecules in the gas phase,[19] the following results are obtained: The ionization pattern recorded at room temperature provides no evidence of a hydroxy isomer[64a] (Figure 17). The decomposition starts above 770 K, as revealed by the appearance of the characteristic sharp peak at 12.6 eV corresponding to the first vertical H_2O ionization. Undecomposed dimethylphosphane oxide can be removed by inserting a 230 K cold trap, so that the bands of H_2O and the dehydration product $H_3C\text{-}P=CH_2$ (Figure 16) dominate the spectrum. Above 970 K, methane is eliminated to form $H\text{-}C\equiv P$ (Figure 17), as observed earlier.[17]

The thermal decomposition of dimethylphosphane oxide thus results in water elimination! By carrying out this novel preparation of 2-phosphapropene on finely granulated silica, for example, the reaction can be optimized[22] and even made superior to the HCl elimination from dimethylchlorophosphane, which needs finely tuned reaction conditions and affords only moderate yields.[22] Condensation of the highly reactive 2-phosphapropene in a 77 K cold trap and careful fractional reevaporation allows, for example, the head-to-tail dimer, trans-1,2-dimethyl-1,3.diphosphetane, to be characterized by mass and PE spectroscopy,[22,64b] and a viscous, glassy polymeric residue is obtained as the main product.

6.3. Electronic Structure of $H_3C\text{-}P=CH_2$: An Ylide with Two-Coordinate P?

Of particular interest is the electron distribution in $H_3C\text{-}P=CH_2$ as revealed by MNDO calculations (19) and experimentally supported by a comparison of its PE spectroscopically determined radical cation states with those of chemically related trimethyl(methylene)phosphorane $(H_3C)_3P=CH_2$,[2,8] the simplest known phosphorus ylide, and the isosteric methyl(methylene)amine $H_3C\text{-}N=CH_2$:[21,65]

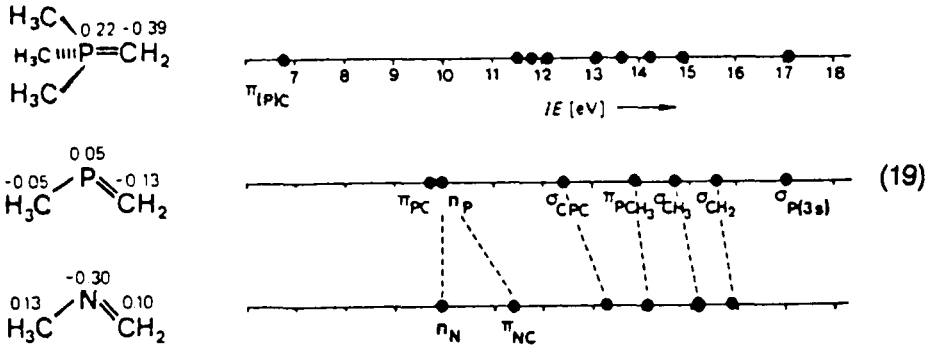

(19)

The PE spectra of all P ylides contain a single band at low ionization energy between 5.95 and 6.85 eV,[2,8] which is assigned to electron removal from the polar $P^{\delta\oplus}{-}C^{\delta\ominus}$ bond exhibiting a relatively high negative charge density at the C atom (19). In contrast, the first ionization of $H_3C\text{-}P{=}CH_2$ is observed only at 9.69 eV and its PE spectrum (Figures 16 and 17) looks very similiar to that of $H_3C\text{-}N{=}CH_2$[65] (19). The change of the $M^{\cdot\oplus}$ sequence $\pi_{PC} < n_P \Rightarrow n_N < \pi_{NC}$ results both from the higher negative charge at the nitrogen center and the wider angle ∢ CNC compared to ∢ CPC in $H_3C\text{-}P{=}CH_2$.[22] The calculated charge densities (19) suggest that the four-coordinate ylide phosphorus contributes much less to the π delocalization than the two-coordinate phosphorus in $H_3C\text{-}P{=}CH_2$. This new molecule, therefore, is best characterized as being a 2-phosphapropene and not an ylide.

6.4. Approximate Energy Hypersurface Caluclation and Chemical Activation

In sharp contrast to the tremendous speed and success, with which phosphorus compounds - being part of the frequently quoted 'renaissance' of main group element chemistry - are presently explored, it remains largely unknown so far how actually medium-sized molecules with n atoms and 3n - 6 degrees of freedom do react.[5] Information needed for the description of microscopic reaction pathways comprise, inter alia, from which directions the molecules involved and energetically 'hot' from preceding collisions, must approach each other for successful penetration and formation of the transition complex, how their structures change during the energy transfer between them and what rôle molecular dynamics plays in this process. The 3 examples selected within the context of gasphase reactions of phosphorus compounds

- ▷ the $P_4 \rightleftarrows 2P_2$ equilibrium (chapter 5 and Figure 15),
- ▷ the thermal HCl elimination $H_3C\text{-}H_2C\text{-}PCl_2 \rightarrow H_3C\text{-}HC{=}P\text{-}Cl \rightarrow H_3C\text{-}C{\equiv}P$ (chapter 2 and Figures 5 and 18), and
- ▷ the thermal dehydration $(H_3C)_2HP{=}O \rightarrow H_3C\text{-}P{=}CH_2$ (chapter 6.3 and Figure 20).

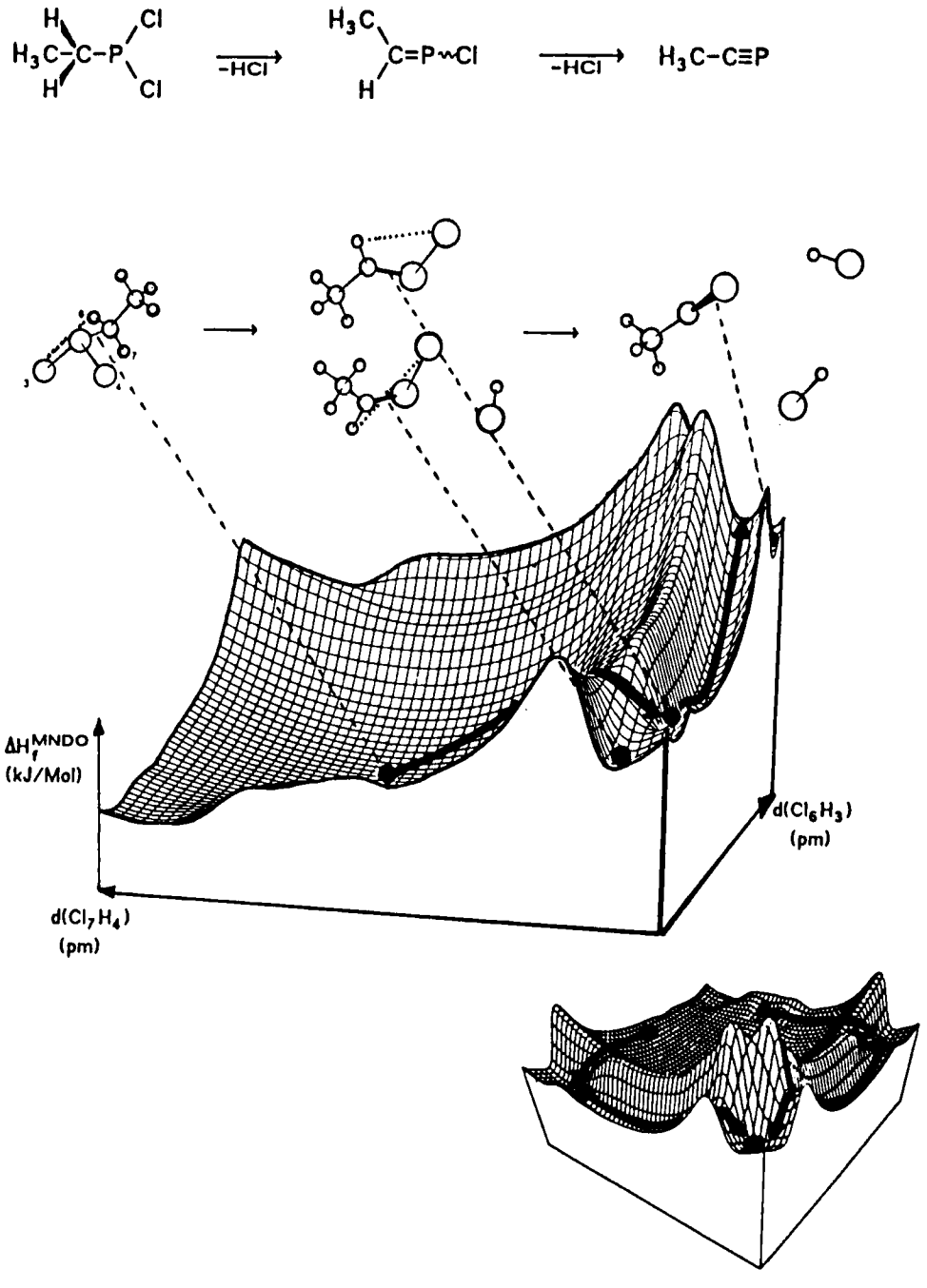

FIGURE 18. MNDO enthalpy of formation hypersurface cut for the thermal HCl elimination from gauche ethyldichlorophosphane to (E) or (Z) H_3C-HC=PCl and to H_3C-C≡P as well as their MNDO geometry-optimized structures (cf. Figure 5). For the reaction profile (●→) cf. (20) and for its discussion see text.

shall illustrate how little we know[5], and how some progress might be achieved[5] both by the skillful preparative chemist hunting and detecting reactive intermediates[19] e.g. by their spectroscopic fingerprints and by approximate hypersurface calculations[20,21] using everywhere available semiempirical programs.[50]

As concerns the thermal two-step HCl elimination from ethyldichlorophosphane (Figure 6), also chosen as model reaction for screening and fine-tuning the heterogeneous catalyst [$MgCl_2$-MgO/SiO_2] (Figures 7 and 8), preliminary calculations already revealed that the enthalpy difference between its slightly more stable gauche and its trans isomer is rather small (Figure 5). For an approximate energy hypersurface calculation, advantageously, the distance parameters d(Cl_3···H_6) and d(Cl_4···H_7) are selected from the $\binom{24}{2}$ = 276 pair combinations to define a cut through the 24-dimensional 'hypersuface' resulting from the 3 · 9 - 6 = 24 degrees of freedom of the 9 atomic molecule H_3C-H_2C-PCl_2.[22] The resulting MNDO hypersurface (Figure 18) includes the enthalpies of formation of all H_3C-H_2C-PCl_2 and H_3C-HC=PCl isomers as well as of the eliminated HCl molecules. Evidently, the starting molecule H_3C-H_2C-PCl_2 can move around in a shallow basin, which reproduces its conformational flexibility. The HCl split-off is more conveniently discussed by following the reaction profile (Figure 18):

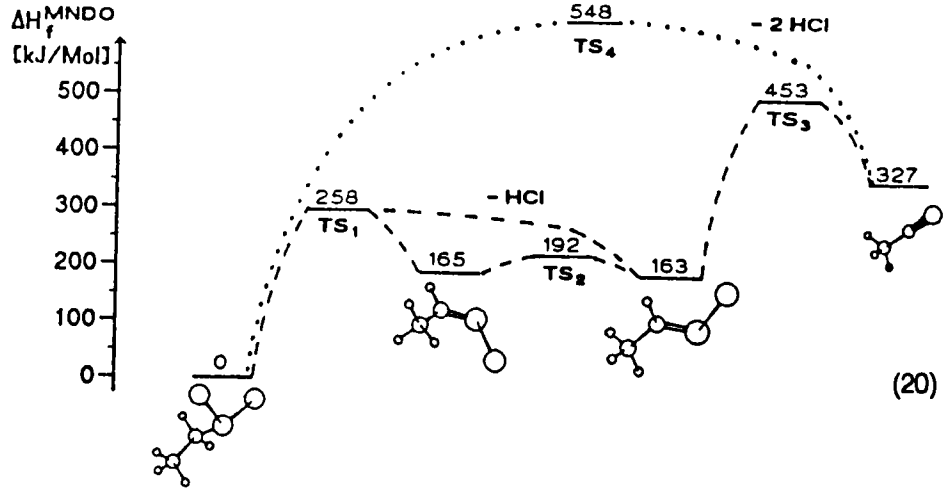

(20)

The (E) and (Z) isomers of H_3C-HC=PCl are formed by HCl extrusion via the same transition state TS_1 representing an activation barrier of 259 kJ/mol. The isomerization barrier of only 27 kJ/mol between them suggests that both are in thermal equilibrium especially at higher temperatures, with the (Z) isomer predicted to be slightly ($\Delta\Delta H_f^{MNDO}$ ~ 2kJ/mol) more stable (cf. Figure 5). The activation barrier of the second HCl elimination along the potential well parallel to the selected reaction coordinate d(Cl_6 ··· H_3) and leading to the second transi-

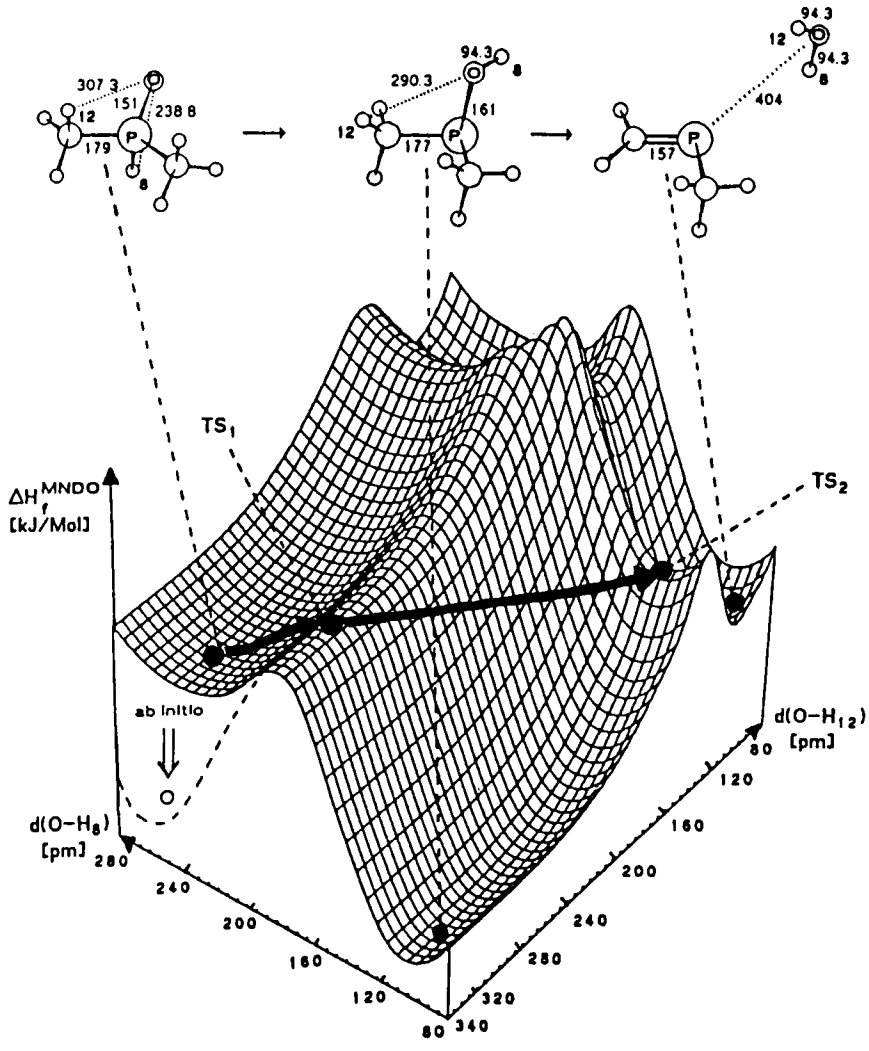

FIGURE 19. Section of the two-parameter MNDO hypersurface for the isomerization of dimethylphosphane and the H_2O elimination to $H_3C\text{-}P{=}CH_2$, as well as MNDO-optimized structures of these compounds (O: value extrapolated from ab initio calculations, cf. text). The reaction profile (●⟶) via the transition states TS_1 and TS_2 is displayed in (21).

tion state TS_2 (Figure 18) amounts to 298 kJ/mol i.e. is only 40 kJ/mol higher than the first one 'up hill' to TS_1. In contrast, for a synchronous expulsion of both HCl leaving molecules to $H_3C\text{-}C{\equiv}P$, 548 kJ/mol are calculated by MNDO, implying that such a double split-off is energetically unfavorable and, therefore, rather unlikely. Altogether, the full approximate MNDO energy hypersurface (Figure 18: additional insert) and the minimum energy reaction pathway (20) inspire the expectation that HCl elimination from ethyldichlorophosphane should

produce a (E) + (Z) isomer mixture of the reactive intermediate $H_3C\text{-}HC{=}PCl$, which can be isolated by cold-trapping and fractionate reevaporation (chapter 2.3 and Figure 9).

The third example selected for a more detailed discussion of its presumable microscopic pathway is the surprising dehydration of dimethylphosphane oxide (Figure 17), which represents an unprecedented type of reaction in organophosphorus chemistry.[60] To rationalize this unexpected observation, a section of the respective MNDO hypersurface (Figure 19) has been calculated, which, by appropriate choice of the coordinates $d(O\cdots H_8)$ and $d(O\cdots H_{12})$ from the total of (3 x 11 - 6) = 27 degrees of freedom, contains the two isomers of the starting material, $(H_3C)_2HP{=}O$ and $(H_3C)_2P\text{-}OH$, as well as the two products, $H_3C\text{-}P{=}CH_2$ and H_2O. With respect to the assumptions introduced,[66] these calculations afford the following speculative insights into the thermolysis pathway, as more conveniently discussed by the reaction profile (Figure 19:●⟶):

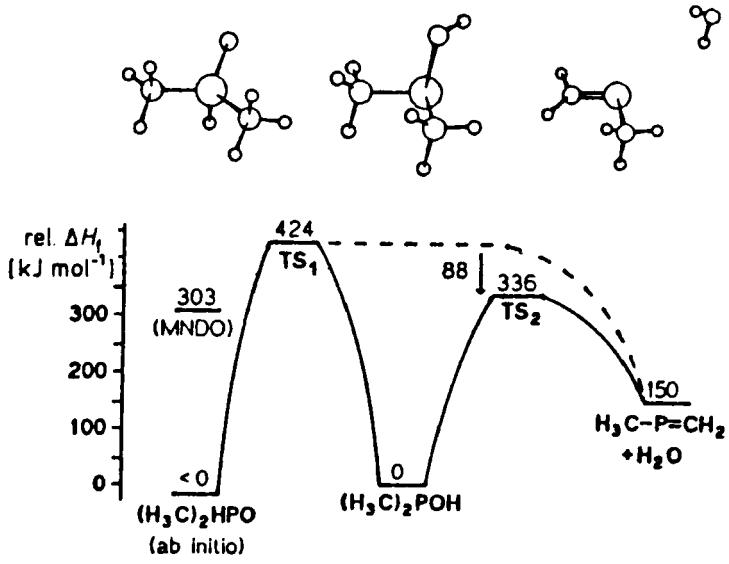

(21)

The MNDO enthalpies of formation (21) suggest a relatively shallow potential well for dimethylphosphane oxide, which is considerably deepened by including d-polarization functions in an ab initio basis set (Figure 19: O). The barrier for the isomerization $(H_3C)_2P\text{-}OH \xrightarrow{\sigma} (H_3C)_2HP{=}O$, calculated by MNDO to amount to approximately 420 kJ/mol, agrees with reported values.[67] The minimum energy reaction pathway crosses the first and highest-energy transition state TS_1 and then follows the slope of the hypersurface to the saddle point TS_2 for the 1,2-HOH elimination at 88 kJ/mol lower energy (21).

The overall endothermic H_2O elimination is apparently preferred over the energetically more favorable isomerization because of the entropy increase. Considering the numerous approximations and, in particular, the selection

among the many degrees of freedom, the reaction profile (21) is also in agreement with the experimental result that not even traces of the possible isomerization product $(H_3C)_2P$-OH are revealed by PE spectroscopy. Under the nearly unimolecular thermolysis conditions (pressure 10 Pa), obviously, only the simultaneous elimination of water allows an effective dissipation of the activation energy stored in the "chemically activated" $(H_3C)_2P$-OH.[68]

This type of reaction, in which unsaturated phosphorus(III) compounds are prepared by thermal elimination of water from phosphane oxides, can be extended to other derivatives.[22] For example, methylphosphinic acid, on gas-phase thermolysis at 820 K

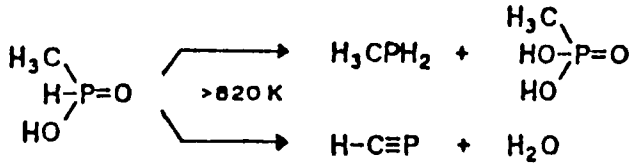

(22)

only partially disproportionates to methylphosphane and methylphosphonic acid, while phosphaacetylene is formed in approximately the same yield by water elimination.[22]

7. CONCLUDING REMARKS: WHAT DOES THE PREPARATIVE CHEMIST BENEFIT FROM CONTEMPLATING MOLECULAR STATE FINGERPRINTS?

Within this report on gasphase investigations of phosphorus compounds, the following reactions in a horizontal flow reactor (Figure 5), have been optimized using their changing photoelectron ionization fingerprints:

▷ the heterogeneously catalyzed dehydrohalogenation of alkyldichlorophosphanes (chapter 2 and Figures 5 to 9):

$$RH_2C{-}PCl_2 \xrightarrow[-HCl]{[MgCl_2\text{-}MgO/SiO_2]} RHC{=}PCl \xrightarrow[-HCl]{[MgCl_2\text{-}MgO/SiO_2]} R{-}C{\equiv}P \quad (23)$$

▷ the dechlorination of alkyldichlorophosphanes at a magnesium metal surface (chapter 3 and Figure 9)

$$R{-}PCl_2 \xrightarrow[-[MgCl_2]]{[Mg]} (RP{\rightarrow}Mg) \begin{cases} \rightarrow (RP)_5 \\ \rightarrow R_3P + R_2P - PR_2 \\ \rightarrow RH \end{cases} \quad (24)$$

▷ the dechlorination of $OPCl_3$ and $SPCl_3$ at silver wool (chapter 4.1 and Figure 11)

$$E=PCl_3 \xrightarrow[-2[AgCl]]{Ag} E=P-Cl \quad (E=O,S) \tag{25}$$

▷ the gasphase dissociation of phosphorus acid chloride pyridinium betaines (chapter 4.2 and Figure 12)

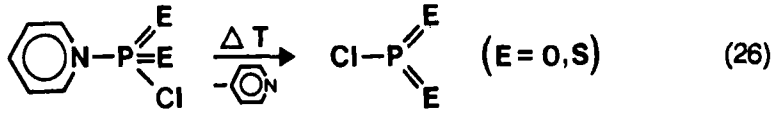

(26)

▷ the gasphase equilibrium of white phosphorus vapor (chapter 5.1 and Figure 14):

$$P_4 \rightleftharpoons 2\ P_2 \tag{27}$$

▷ and thermolysis reactions yielding 2-phosphapropene (chapter 6 and Figures 16 and 17):

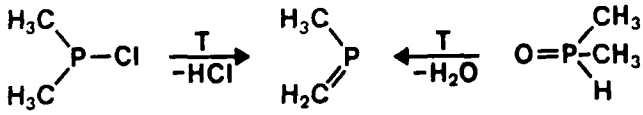

(28)

In addition, the photoelectron ionization fingerprints used for the real-time gas analysis in the flow systems, have been assigned to radical cation state sequences via Koopman's theorem, $IE_n^V = -\varepsilon_J^{SCF}$ based on MNDO and ab initio calculated eigenvalues $-\varepsilon_J^{SCF}$. This allows to unequivocally identify and characterize both the starting materials and especially the novel unsaturated phosphorus compounds generated thermally or catalytically under nearly unimolecular conditions i.e. preventing oligomerization of the reactive intermediates by reducing the pressure in the gas flow. The PE spectroscopic assignments comprise:

- ▷ $H_3CH_2C\text{-}PCl_2$ (Figure 5),
- ▷ $H_2C=PCl$, $H_3C\text{-}HC=PCl$ and $(H_3C)_2C=PCl$ (Figure 9),
- ▷ O=P-Cl and S=P-Cl (Figure 11),
- ▷ $Cl\text{-}P(=O)_2$ and $Cl\text{-}P(=S)_2$ (Figures 12 and 13),
- ▷ P≡P (Figure 14), and
- ▷ $H_3C\text{-}P=CH_2$ (Figure 16).

Correlating measurements and calculations, many other properties of molecular states (Figure 1) can be rationalized (Figure 3). As concerns the phosphorus compounds, the chemistry of which is indicated in equations (23) to (28), numerous structures have been calculated for their respective minima of total energy, e.g. for $H_3CH_2C\text{-}PCl_2$ (Figures 5 and 18), for $H_3C\text{-}HC=PCl$ and

$H_3C\text{-}C\equiv P$ (Figure 18), for Cl-P=O and Cl-P=S (Figure 11), for $Cl\text{-}P(=O)_2$ and $Cl\text{-}P(=S)_2$ (Figures 12 and 13), for $H_3C\text{-}P=CH_2$ (Figures 18 and 19) as well as for $(H_3C)_2HP=O$ and $(H_3C)_2POH$ (Figure 19). Charge distributions are given, inter alia for Cl-P=O (9), for $Cl\text{-}P(=O)_2$ and $Cl\text{-}P(=S)_2$ (Figure 13) or for $H_3C\text{-}P=CH_2$ (13).

As concerns the much emphasized comparison of equivalent states of chemically related compounds (Figure 4), methyl perturbation of $H_2C=PCl$ (Figure 9) provides insight into to electron distribution of the $\pi_{C=P}$ bond and the ionization potentials. Total and π charges for the series of planar 4 atom/24 electron molecules Cl_3B ... $Cl_2C=S$ ... $Cl\text{-}P(=S)_2$ ... $Cl\text{-}P(=O)_2$ ...$Cl\text{-}N(=O)_2$ .... SO_3 reveal similarities and differences in their electronic structures (Figure 13). For $H_3C\text{-}P=CH_2$, molecular state comparison (19) allows the clear-cut statement, that this novel molecule is not an ylide but a 2-phosphapropene.

Last but not least, facets of the molecular dynamics of medium-sized phosphorus compounds with their presently still untreatable 3n - 6 degrees of freedom and, above all, facets of their microscopic reaction pathways are discussed, based on numerous simplyfing assumptions and approximations. Pointing out these inherent limitations, energy hypersurface cuts calculated for selected molecular dynamics coordinates are presented for the following gasphase thermolysis reactions:

- the $P_4 \rightleftarrows 2\ P_2$ equilibrium (Figure 15),
- the dehydrochlorinations $H_3C\text{-}H_2C\text{-}PCl_2 \longrightarrow H_3C\text{-}HC=PCl \longrightarrow H_3C\text{-}C\equiv P$ (Figure 18, and
- the dehydration $(H_3C)_2HP=O \longrightarrow H_3C\text{-}P=CH_2$ (Figure 19).

The careful discussion of potential topological reaction possibilities (16) or the reaction profiles (20) or (21) reveal, how little we actually know about the rather complex processes involved in seemingly simple gasphase fragmentations, but also, how experimental results might at least be rationalized. Thus the non-observability of the tautomer $(H_3C)_2P\text{-}OH$ (Figure 17) within the measurement time-scale of ~ 10^{-4} seconds agrees well with the suggestion from the approximate hypersurface calculation (Figure 19) that the microscopic reaction pathway might include a 'chemically activated' intermediate (chapter 6.4.).

Altogether and returning to the initial question, of what a preparative phosphorus chemist can benefit from 'looking' at his daily efforts to further explore and extend his fascinating area of research by using the 'molecular state magnifier' (Figure 2), the answer is 'more than he might assume at first sight' or - quoting nobel laureate Wilhelm Ostwald - 'the practician distinguishes himself from a theoretician just by stopping earlier to ask questions'.[69]

REFERENCES

1. Essay 21 on Molecular Properties and Models. For essay 20 on 'Principles of Silicon Chemistry - Molecular States of Silicon Containing Molecules' cf. Angew. Chem. 101 (1989), in print.
2. Cf. the first report on 'Photoelectron Spectra and Bonding in Phosphorus Compounds', H. Bock, Lecture Abstr. 2nd IUPAC Symposium on Phosphorus Compounds, Prague; Pure Appl. Chem. 44, 343 - 372 (1975).
3. Cf. also H. Bock 'Molecular States and Molecular Orbitals', Angew. Chem. 89, 631 (1977); Angew. Chem. Int. Ed. Engl. 16, 613 (1977) and literature cited.
4. Cf. e.g. E. Heilbronner and H. Bock 'The HMO Model and its Application', Verlag Chemie Weinheim 1969, Japanese Translation: Hirokowa Tokyo 1973, English Translation: Wiley & Sons London 1976 and Chinese Translation: Kirin Univ. Press (China) 1982; especially Vol. 1., chapters 6 and 7.
5. Cf. e.g. H. Bock 'What do We Actually Know about Reaction Pathways?', Polyhedron 7, 2429 (1988) and literature quoted. See also H. Bock, Österr. Chem. Z. 1989/5, 142 or L'actualite Chim. 3, 33 (1986).
6. An essay analogous to[1] on 'Molecular States of Phosphorus Containing Molecules', will be submitted to Angew. Chem. for publication.
7. H. Bock, G. Rudolph, E. Baltin and J. Kroner, Angew. Chem. 77, 469 (1965); Angew. Chem. Int. Ed. Engl. 4, 457 (1965) and Lit.cit.; cf. also H. Bock, K. Wittel, M. Veith and N. Wiberg, J. Am. Chem. Soc. 98, 109 (1976).
8. K.A. Ostoja Starzewski and H. Bock, J. Am. Chem. Soc. 98, 8486 (1976) as well as K.A. Ostoja Starzewski, H. Bock and H. tom Dieck, Angew. Chem. 87, 197 (1975); Angew. Chem. Int. Ed. Engl. 14, 173 (1975) and J. Organomet. Chem. 65, 311 (1974).
9. H. Bock, B. Solouki, G. Fritz and W. Hölderich, Z. anorg, allg. Chem. 458, 53 (1979). See also H. Bock, A. Semkow and M. Baudler, unpublished results.
10. H. Bock, U. Lechner-Knoblauch and P. Hänel. Chem. Ber. 119, 3749 (1986).
11. H. Bock, B. Hierholzer and D. Jaculi, Z. Naturforsch. 43b, 1247 (1988), W. Kaim, U. Lechner-Knoblauch, P. Hänel and H. Bock, J. Org. Chem. 48, 4206 (1983), W. Kaim, H. Bock and H. Noeth, Chem. Ber. 111, 3276 (1977).
12. F. Gerson, G. Plattner and H. Bock, Helv. Chim. Acta 53, 1629 (1970), W. Kaim, P. Hänel and H. Bock, Z. Naturforsch. 37b, 1382 (1982) or W. Kaim, P. Hänel, U. Lechner-Knoblauch and H. Bock, Chem. Ber. 115, 1265 (1982).

13. H. Bock and M. Bankmann, Phosphorus, Sulfur, Silicon Rel. Elements, in print; for other alkylidene phosphanes like $R_3Si\text{-}C{=}P$ cf. B. Solouki, H. Bock, R. Appel, A. Westerhaus, G. Becker and G. Uhl, Chem. Ber. 115, 3747 (1982).
14. H. Bock and H. Müller, Inorg. Chem. 23, 4365 (1984).
15. M. Binnewies, B. Solouki, H. Bock, R. Becherer and R. Ahlrichs, Angew. Chem. 96, 704 (1984); Angew. Chem. Int. Ed. Engl. 23, 731 (1984).
16. M. Meisel, H. Bock, B. Solouki and M. Kremer, Angew. Chem. 101 (1989), in print.
17. H. Bock and M. Bankmann, Angew. Chem. 98, 287 (1986); Angew. Chem. Int. Ed. Engl. 25, 265 (1986).
18. H. Bock and M. Bankmann, Angew. Chem. 101 (1989), in print.
19. Cf. the summary by H. Bock, B. Solouki, S. Aygen, M. Bankmann, O. Breuer, R. Dammel, J. Dörr, M. Haun, T. Hirabayashi, D. Jaculi, J. Mintzer, S. Mohmand, H. Müller, P. Rosmus, B. Roth, J. Wittmann and H.P. Wolf, J. Mol. Structure, 173, 31 (1968) and lit.cit.
20. Cf. H. Bock, R. Dammel and B. Roth 'Molecular State Fingerprints and Semiempirical Hypersurface Calculations: Useful Correlations to Track Short-Lived Molecules' in ACS Special Report 'Inorganic Rings and Clusters', ACS Symposium Series 232, 139, (1983) and lit.cit.
21. Cf. also H. Bock and R. Dammel, Angew. Chem. 99, 518 (1987); Angew. Chem. Int. Ed. Engl. 26, 504 (1987).
22. Unpublished results, cf. Ph.D. thesis M. Bankmann, University of Frankfurt 1989.
23. H. Bock and B. Solouki, Angew. Chem. 93, 425 (1981); Angew. Chem. Int. Ed. Engl. 20, 427 (1981).
24. Cf. e.g. the heterogeneously catalyzed reaction of benzene with NCCN (H. Bock, J. Wittmann and H.J. Arpe, Chem. Ber. 115, 2326 (1982)) or the gasphase bromination of trifluoromethane (H. Bock, J. Wittmann, J. Mintzer and J. Russow, Chem. Ber. 115, 2346 (1982)).
25. For preceding investigations on alkylidene phosphanes $R\text{-}C{=}P$ cf. e.g.[13] and the literature summarized therein. H.W. Kroto reviews his contributions in Chem. Soc. Rev. 11, 435 (1982).
26. Recently, S. Lacombe, D. Goubeau, J.-L. Cabioch, B. Pellerin, J.-M. Denis and G. Pfister-Guillozo (J. Am. Chem. Soc. 110, 6964 (1988) reported the use of solid K_2CO_3 at 373 K to eliminate HCl from chloroalkylphosphanes.
27. B. Pellerin, J.-M. Denis, J. Perrocheau and R. Carrie, Tetrahedron Lett. 27, 5723 (1986).
28. M. Beez, G. Bieri, H. Bock and E. Heilbronner, Helv. Chim. Acta 56, 1028 (1973).
29. H. Bock and W. Kaim, Chem. Ber. 111, 3552 (1978).
30. Cf. e.g. the review by J.I.G. Cadogan and P.K.G. Hodgson, Phosphorus and Sulfur 30, 3 (1987) and lit.cit.

31. Cf. e.g. (a) R = $C_6H_2(C(CH_3)_3)_3$: M. Yoshifuji, I. Shima, N. Inamato, K. Hirotsu and T. Higuchi, J. Am. Chem. Soc. 103, 4587 (1981); (b) R = $C(Si(CH_3)_3)_3$: A.H. Cowley, J.E. Kilduff, T.H. Newmann and M. Pakulski, J. Am. Chem. Soc. 104, 5820 (1982) or R = $C_5(CH_3)_5$: P. Jutzi, U. Meyer, B. Krebs and N. Dartmann, Angew. Chem. 98, 894 (1986), Angew. Chem. Int. Ed. Engl. 25, 919 (1986).
32. Cf. e.g. H.F. Grützmacher, W. Silhan and U. Schmidt, Chem. Ber. 102, 3250 (1969) as well as U. Schmidt, I. Boie, C. Osterroth, R. Schröder and H.F. Grützmacher, ibid. 101, 1381 (1968) and lit.cit.
33. M.T. Nguyen, M.A. McGinn and A.F. Hegarty, Inorg. Chem. 25, 2185 (1986).
34. K.S. Root, J. Dentsch and. G.M. Whitesides, J. Am. Chem. 103, 5475 (1981).
35. R.G. Nuzzo and L.H. Dubois, J. Am. Chem. Soc. 108, 2881 (1986).
36. Cf. e.g. [21] and especially Ph.D. Thesis H.P. Wolf, University of Frankfurt 1988, p. 46-82.
37. Cf. e.g. H. Bock and O. Breuer, Angew. Chem. 99, 492 (1987), Angew. Chem. Int. Ed. Engl. 26, 461 (1987).
38. M. Binnewies, Thermochim. Acta 67, 387 (1983); M. Binnewies, M. Lakenbrink and H. Schnöckel, Z. Anorg. Allg. Chem. 497, 7 (1983); M. Binnewies, ibid. 505, 77 (1983) as well as 507, 32 and 66 (1983). Cf. also E. Lindner, K. Auch, W. Hiller and R. Fawzi (Angew. Chem. 96, 287 (1984); Angew. Chem. Int. Ed. Engl. 23, 320 (1984), who trapped a thioxophosphane intermediate in the dehalogenation of dichloro(methyl)thioxophosphorane with by adding of $Mn_2(CO)_{10}$.
39. A.D. Walsh, J. Chem. Soc. 1953, 2266. Cf. also R.J. Buenker and S.D. Peyerimhoff, Chem. Rev. 74, 127 (1974), and B.M. Gimarc, J. Am. Chem. Soc. 100, 2346 (1978) as well as each literature cited.
40. For the assignment of the PE spectra of phosphorus halides like $Cl_3P{=}S$ or Cl_3P cf. K. Wittel and H. Bock in 'The Chemistry of Functional Groups, Suppl. D' (ed. S. Patai and Z. Rappoport). Wiley, London 1983, p. 1560 f. and literature cited.
41. H. Bock, S. Aygen, P. Rosmus, B. Solouki and E. Weißflog, Chem. Ber. 117, 187 (1984).
42. R. Ahlrichs, C. Ehrhardt, M. Lakenbrink, S. Schunk and H. Schnöckel, J. Am. Chem. Soc. 108, 3596 (1986) and literature quoted. For Cl-P=O cf.[15].
43. Cl-$P(=O)_2$: G.U. Wolf and M. Meisel, Z. Chem. 22, 54 (1982); Cl-$P(=S)_2$: M. Meisel and H. Grunze, Z. anorg. allg. Chem. 360, 277 (1968) and lit.cit.
44. Cf. A.F. Wells 'Structural Inorganic Chemistry', 4th Edit., Clarendon Press, Oxford 1975. For $Cl_2C{=}S$ cf. N. Nakata, T. Fukuyama and K. Kichutsu, J. Mol. Structure 81, 121 (1982).

45. H. Bock, B. Solouki and M. Binnewies, unpublished results.
46. Cf. e.g. "Gmelin Handbuch der Anorganischen Chemie: Phosphorus", Vol. B-8, Verlag Chemie, Weinheim, 1964. For P = 0.19 and T = 1370 K the values α = 0.41 and ln $K_P/4$ = -0.81 are reported.
47. B.J. McBride, S. Heimel, J.G. Ehlers and S. Cordon. NASA [Spec. Publ.] SP NASA SP-3001, 257.
48. C.R. Brundle, N.A. Kuebler, M.B. Robin and H. Basch, Inorg. Chem. 11, 20 (1972). Cf. also S. Evans, P.J. Joachim, A.F. Orchard and D.W. Turner, Int. J. Mass Spectrom. Ion. Phys. 9, 41 (1972); M.F. Guest, I.H. Hillier and V.R. Saunders. J. Chem. Soc., Faraday Trans. 2 68, 2070 (1972); D.K. Bulgin, J.M. Dyke and A. Morris. J. Chem. Soc., Faraday Trans. 2 72, 2225 (1976) or D.P. Chong and Y. Takahata, J. Electron Spectrosc. Relat. Phenom. 10, 137 (1977). For the first report of P_2 see A.W. Potts, K.G. Glenn and W.A. Price. Faraday Discuss. Chem. Soc. 1972, 65.
49. For gas-phase reactions of P_4 and P_2 cf. H. Bock, H. Wittmann and H. Müller, Chem. Ber. 115, 2338 (1982).
50. M.J.S. Dewar and W. Thiel, J. Am. Chem. Soc. 99, 5899 (1977).
51. R. Osman, P. Coffey and J.R. van Wazer, Inorg. Chem. 15, 287 (1976).
52. R.G. Pearson "Symmetry Rules for Chemical Reactions"; Wiley Interscience: New York 1976; p 62 f. and 117. For the C_4H_4 hypersurface see H. Kollmar, F. Carrion, M.J.S. Dewar and R.C. Bingham, J. Am. Chem. Soc. 103, 5292 (1981). Cf. also the opening of the tetrahedrane $(RC)_4$ cluster: H. Bock, B. Roth and G. Maier, Angew. Chem. 92, 213 (1980), Angew. Chem. Int. Ed. Engl. 19, 209 (1980) as well as Chem. Ber. 117, 172 (1984).
53. Cf. e.g. U. Wedig, H. Stoll and H. Preuss, Chem. Phys. 61, 117 (1981).
54. E.A. Halevi, Angew. Chem. 88, 664 (1976); Angew. Chem. Int. Ed. Engl. 15, 593 (1976). Cf. also the report on the symmetry-forbidden dimerization $2P_4 \rightleftarrows P_8$: E.A. Halevi, H. Bock and B. Roth, Inorg. Chem. 23, 4369 (1984).
55. Cf. the review by O.J. Scherer on "Phosphorus, Arsenic, Antimony, and Bismuth Multiply Bonded Systems with Low Coordination Number - Their Role as Complex Ligands" (Angew. Chem. 97, 905 (1895); Angew. Chem. Int. Ed. Engl. 24, 924 (1985) and references cited therein.
56. M.J. Hopkinson, H.W. Kroto, J.F. Nixon and N.P. Simmons, J. Chem. Soc. Chem. Commun. 1976, 513. Gasphase structure: B. Bak, N.S. Kristiansen and H. Svanholt, Acta Chem. Scand. Ser. A36, 1 (1982). In the mean-time, the synthesis has also been achieved by reaction of gaseous H_3CPI_2 with solid KOR, and the isolated compound could be characterized by NMR spectroscopy at 260 K: R. Carrie and J.-M. Denis (University Rennes), Abstr. CNRS Colloquium la Tour de Carol, May 1985.

57. Cf. the review by H. Bock and B.G. Ramsey on 'PE Spectra of Main Group Element Compounds', Angew. Chem. 85, 773 (1973); Angew. Chem. Int. Ed. Engl. 12, 734 (1973).

58. D.H. Aue, H.M. Webb, W.R. Davidson, M. Vidal, M.T. Bowers, H. Goldwhite, L.E. Vertal, J.E. Douglas, P.A. Kollmann and G.L. Kenyon, J. Am. Chem. Soc. 102, 5151 (1980).

59. Cf. also M. Regitz and P. Binger, Angew. Chem. 100, 1541 (1988); Angew. Chem. Int. Ed. Engl. 27, 1484 (1988) or K. Karaghiosoff and A. Schmidtpeter, Phosphorus Sulfur 36, 217 (1988).

60. A careful literature search revealed that cyclohexyl- and (3-pentyl)phosphane oxides upon heating at 60°C/1 torr, afford mixtures of products, from which tetraalkyltetraphosphetanes, $(RP)_4$, can be isolated in small yields (W.M.A. Henderson, Jr., M. Epstein and F.S. Seichter, J. Am. Chem. Soc. 85, 2462 (1963).

61. Cf., e.g. the Scientific Symposium "125 Jahre Hoechst", Festschrift Hoechst AG 1989, p. 72.

62. Cf. J.E. Huheey 'Inorganic Chemistry: Principles of Structure and Reactivity', Harper and Row, New York 1978, p. 839f.

63. Calculations for substituted phosphane oxides XYHP=O with X,Y = H, CH_3, NH_2, OR, F (M.S. Gordon, J.A. Boatz and M.W. Schmidt, J. Phys. Chem. 88, 2998 (1984); ibid. 91, 1743 (1987)) suggest that the oxo forms are usually more stable than the hydroxy isomers XYP-OH and that the activation barrier for the isomerization $H_3P{=}O \rightarrow H_2POH$ should amount to approximately 300 kJ mol^{-1}. Elimination of HX or XY has been proposed as a possible thermolysis pathway. Experimentally, the hydroxy form has been observed only for acceptor-substituted derivatives like (F_3C_2)P-OH (J.E. Griffith and A.B. Burg, J. Am. Chem. Soc. 84, 3442 (1962)) or on complex stabilization, e.g., in $[(OC)_4HalMn \leftarrow PR_2OH]$ (E. Lindner and B. Schilling, Chem. Ber. 110, 3266 (1977)).

64. Vertical ionization energies of $(CH_3)_2HP{=}O$ with assignment:[22] 10.32 eV (n_O, $\pi_{P=O}$), 12.9 eV(σ_{PC}, σ_{PH}, σ_{PO}), and > 14.5 eV (σ_{CH}). For trans-1,3-dimethyl-1,3-diphosphetane: m/z 120 ($M^{\oplus}$), 105 ($M^{\oplus}$-CH_3), 92, 77, 75, 57, 45; IE^V = 8.0 ($4b_g$), 9.3 ($6a_g$), 11.3 ($3b_g$, $3a_u$, $5b_u$), 12.9 - 15.5 eV; ΔH_f(MNDO) = -274.1 kJ mol^{-1}.

65. H. Bock and R. Dammel, Chem. Ber. 120, 1961 (1987) and literature quoted. For the preparatation of methane imines cf. J.C. Giullemin and J.-M. Denis, Angew. Chem. 94, 715 (1982); Angew. Chem. Int. Ed. Engl. 21, 690 (1982) and especially Angew. Chem. Suppl. 1982, 1515 as well as additional references given. For PE spectroscopic investigations see also J.B. Peel and G. Willet, J. Chem. Soc. Faraday Trans. 2 71, 1799 (1975) or D.C. Frost, B. MacDonald, C.A. McDowell and N.P.C. Westwood, J. Electron Spectrosc. Relat. Phenom. 14, 379 (1978).

66. According to the literature, bond enthalpies of four-coordinate phosphorus(V) compounds obtained from MNDO calculations are usually too high, because d-polarization functions are not included in the MNDO parameter set (cf. M.J.S. Dewar, M.L. McKee and H.S. Rzepa, J. Am. Chem. Soc. 100, 3607 (1978). On the other hand, ab initio studies,[63] in agreement with the experimental data, indicate that nearly all derivatives HXYPO are 10 - 60 kJ mol^{-1} more stable than the corresponding tautomers XYPOH. According to the Hammond principle (J. Am, Chem. Soc. 77, 334 (1955)), the transition states of endothermic reactions should be product-like. Since these reactions are endothermic, therefore, the MNDO results of both the isomerization and the H_2O elimination for the phosphorus(III) derivatives satisfactorily approximate this part of the energy hypersurface (Figure 19). For the phosphorus(V) compound $(H_3C)_2HP=O$, the ab initio total energy[63] has also been inserted (Figure: 19: O) to demonstrate that the potential well calculated by MNDO is too shallow.

67. Cf. e.g., M.W. Schmidt, S. Yabushita and M.S. Gordon, J. Phys. Chem. 88, 32 (1984) as well as[63] and C.J. Cramer, C.E. Dykstra and S.E. Denmark, Chem. Phys. Lett. 136, 17 (1987), who calculate isomerization barriers $R_2POH \rightleftharpoons R_2HP=O$ of between 290 and 365 kJ mol^{-1}.

68. For other examples of experimentally verified chemical activation, cf. H. Bock and R. Dammel, Angew. Chem. 90, 518 (1987); Angew. Chem. Int. Ed. Engl. 26, 504 (1987) and references cited therein. The "chemically activated" $H_2C=NH$, generated by methyl azide pyrolysis, eliminates H_2 in the subsequent reaction channel and forms HCN at a temperature 500 K lower than after prior isolation in a 180 K cold trap.

69. Cf. H.-J. Quadbeck-Seeger "Zwischen den Zeichen", VCH Verlagsges. Weinheim 1988.